

Supporting Information

Zn(II)/Ag(I) bi-heterometallic based assemblies with
unexpected highly catalytic activity for the hydrolysis of
phosphodiester

Shuai-Bing Li^a, Ning Liu^a, Yan-Zhen Zheng^{c}, and Jiang-Shan*

Shen^{a,b}*

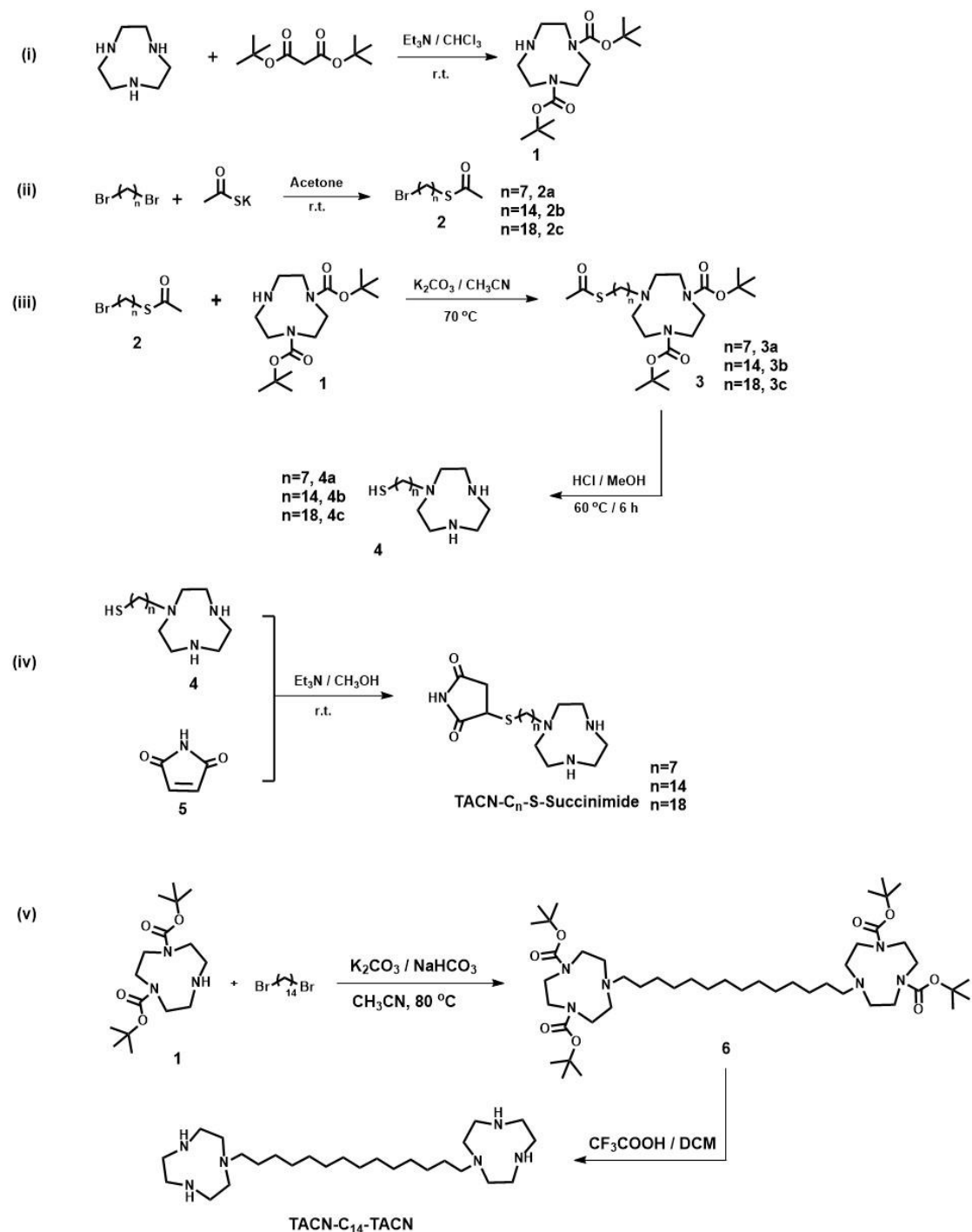
^aCollege of Materials Science and Engineering, Huaqiao University, Xiamen, 361021, China. E-mail: jsshens@hqu.edu.cn

^b Xiamen Key Laboratory of Optoelectronic Materials and Advanced Manufacturing, Huaqiao University, Xiamen, 361021, China.

^cCollege of Ocean Food and Biological Engineering, Jimei University, Xiamen, 361021, China. E-mail: yanzhenzheng@jmu.edu.cn

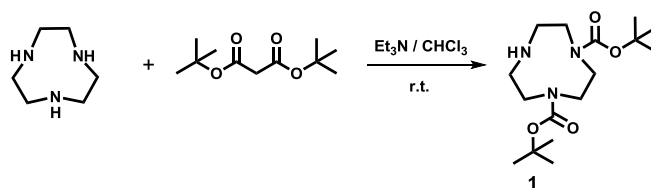
1. Synthesis and characterization of TACN-C_n-S-Succinimide (n=7, 14, and 18), control TACN-C₁₄-TACN, and substrate HPNP

1.1. Synthesis routes of TACN-C_n-S-Succinimide and TACN-C₁₄-TACN



Scheme S1. The synthesis routes of TACN-C_n-S-Succinimide (n=7, 14, and 18; i-iv) and TACN-C₁₄-TACN (i and v).

1.2. Synthesis and characterization of **1**



Scheme S2. The synthesis route of **1**.

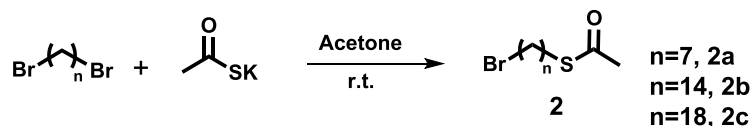
323 mg (2.5 mmol) 1,4,7-triazacyclonane (TACN) was dissolved in 12 mL of chloroform. 3 equiv (750 μ L) triethylamine was slowly injected into above TACN solution under N₂ gas atmosphere. 545 mg (2.5 mmol) bis(1,1-dimethylethyl) ester was dissolved in 4 mL of chloroform, and this solution was slowly injected into the aforementioned TACN solution through an automatic sampler (the flow rate was set to 20 μ L \cdot min⁻¹). The mixed solution was stirred overnight at 25 °C. The crude product was purified by using silica gel column chromatography (eluent: V_{DCM}/V_{Methanol} = 50/1) to obtain 256 mg of **1** colorless oil-like pure compound (**1**) (31.1 % yield).

¹H NMR (500 MHz, CDCl₃) δ (ppm) = 3.43 (d, J = 35.0 Hz, 4H), 3.24 (d, J = 28.8 Hz, 4H), 2.90 (q, J = 5.0, 4.6 Hz, 4H), and 1.45 (s, 18H).

¹³C NMR (126 MHz, CDCl₃) δ (ppm) = 155.99, 155.72, 79.65, 53.40, 53.04, 52.45, 52.31, 51.57, 50.36, 49.78, 49.51, 48.24, 48.08, 47.68, 47.30, and 28.49.

HRMS (ESI-MS) m/z : [M+H]⁺ Calcd. 330.2388; Found: 330.2389.

1.3 Synthesis and characterization of **2**



Scheme S3. The synthesis route of **2**.

1 mmol of 1, n-di-Br-alkanes with different carbon atom number of alkyl chain was dissolved in 5 mL of acetone, and 228.4 mg (1 mmol) potassium thioacetate was slowly added into the alkene solution. The mixed solution was stirred overnight at room temperature. Rotatory evaporation under a vacuum was used to remove the solvent to

afford the crude product. The crude product was purified by using silica gel column chromatography (eluent: $V_{PE}/V_{DCM} = 10/1$) to obtain the pure compound **2(2a-2c)** (56.9 % yield).

2a: $^1\text{H NMR}$ (500 MHz, CDCl_3) $\delta(\text{ppm}) = 3.35$ (t, $J = 6.8$ Hz, 2H), 2.83 - 2.78 (m, 2H), 2.27 (s, 3H), 1.83 - 1.75 (m, 2H), 1.56 - 1.48 (m, 2H), 1.41 - 1.34 (m, 2H), and 1.35 - 1.26 (m, 4H).

$^{13}\text{C NMR}$ (126 MHz, CDCl_3) $\delta(\text{ppm}) = 196.02, 33.89, 32.69, 30.66, 29.40, 29.04, 28.56, 28.24,$ and 27.99.

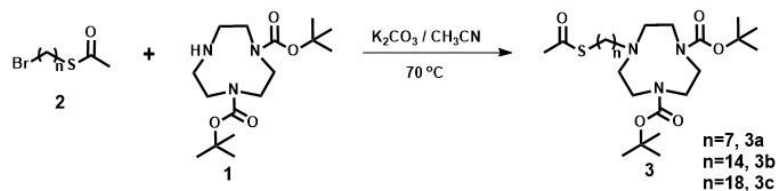
2b: $^1\text{H NMR}$ (500 MHz, CDCl_3) $\delta(\text{ppm}) = 3.42$ (d, $J = 6.9$ Hz, 2H), 2.88 (t, $J = 7.4$ Hz, 2H), 2.35 (s, 3H), 1.87 (dt, $J = 14.5, 7.0$ Hz, 2H), 1.44 (t, $J = 7.4$ Hz, 3H), 1.40 - 1.34 (m, 4H), and 1.27 (s, 16H).

$^{13}\text{C NMR}$ (126 MHz, CDCl_3) $\delta(\text{ppm}) = 196.16, 34.11, 32.85, 30.67, 29.72, 29.60, 29.57, 29.54, 29.51, 29.48, 29.45, 29.18, 29.13, 28.84, 28.78,$ and 28.19.

2c: $^1\text{H NMR}$ (500 MHz, CDCl_3) $\delta(\text{ppm}) = 3.43$ (t, $J = 6.9$ Hz, 2H), 2.88 (t, $J = 7.4$ Hz, 2H), 2.34 (s, 3H), 1.88 (dt, $J = 14.5, 7.0$ Hz, 2H), 1.43 (q, $J = 7.2$ Hz, 2H), 1.37 (t, $J = 7.9$ Hz, 3H), and 1.27 (s, 26H).

$^{13}\text{C NMR}$ (126 MHz, CDCl_3) $\delta(\text{ppm}) = 196.00, 34.00, 32.86, 31.51, 30.63, 30.14, 29.67, 29.66, 29.64, 29.62, 29.58, 29.55, 29.51, 29.48, 29.45, 29.17, 29.13, 28.83, 28.78,$ and 28.19.

1.4. Synthesis of **3**



Scheme S4. The synthesis route of **3**.

3 equiv. of K_2CO_3 , 3 equiv. of NaHCO_3 , and 0.57 mmol of **2** were added to 10 mL

acetonitrile solution containing 0.57 mmol of compound **1**. The mixed solution was stirred overnight at 70 °C. After the solvent was removed using rotary evaporation under a vacuum, the crude product was purified by using silica gel column chromatography (eluent: $V_{PE}/V_{EA} = 10/1$) to obtain the pure compound **3** (**3a-3c**) (71.2 % yield).

3a: ¹H NMR (500 MHz, CDCl₃) δ (ppm) = 3.46 (d, $J = 23.7$ Hz, 4H), 3.25 (d, $J = 18.1$ Hz, 4H), 2.88 - 2.82 (m, 2H), 2.61 (d, $J = 9.1$ Hz, 4H), 2.46 (dt, $J = 15.3, 4.2$ Hz, 2H), 2.32 (s, 3H), 1.55 (d, $J = 7.4$ Hz, 2H), 1.47 (s, 19H), 1.41 (q, $J = 6.9$ Hz, 3H), 1.34 (q, $J = 7.9, 7.2$ Hz, 3H), and 1.30 - 1.24 (m, 4H).

¹³C NMR (126 MHz, CDCl₃) δ (ppm) = 195.38, 155.70, 155.57, 155.40, 79.36, 79.28, 56.92, 56.77, 54.02, 53.61, 50.78, 50.61, 50.42, 50.20, 49.92, 49.75, 49.69, 30.64, 29.69, 29.48, 29.14, 29.10, 29.07, 28.81, and 28.55.

HRMS (ESI-MS) m/z : [M+H]⁺ Calcd. 502.3309; Found: 502.3308.

3b: ¹H NMR (500 MHz, CDCl₃) δ (ppm) = 3.46 (d, $J = 17.0$ Hz, 4H), 3.24 (d, $J = 21.4$ Hz, 4H), 2.86 (t, $J = 7.4$ Hz, 2H), 2.61 (d, $J = 15.1$ Hz, 4H), 2.46 (tt, $J = 6.5, 3.4$ Hz, 2H), 2.33 (s, 3H), 1.55 (q, $J = 7.5$ Hz, 2H), 1.47 (s, 18H), 1.43 - 1.33 (m, 5H), and 1.26 (s, 21H).

¹³C NMR (126 MHz, CDCl₃) δ (ppm) = 195.90, 155.64, 155.49, 155.33, 79.27, 79.19, 56.97, 56.82, 54.02, 53.59, 50.65, 50.55, 50.34, 50.15, 49.96, 49.70, 30.58, 29.64, 29.58, 29.53, 29.47, 29.43, 29.08, 28.77, 28.54, 28.51, 28.07, 27.91, 27.71, 27.51, 27.42, and 27.35.

HRMS (ESI-MS) m/z : [M+H]⁺ Calcd. 600.4405; Found: 600.4403.

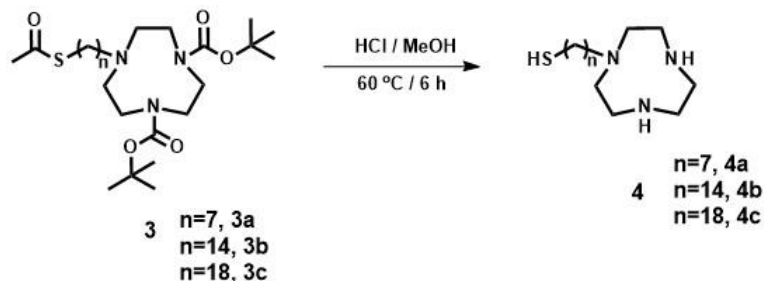
3c: ¹H NMR (500 MHz, CDCl₃) δ (ppm) = 3.46 (d, $J = 22.5$ Hz, 4H), 3.24 (d, $J = 21.7$ Hz, 4H), 2.86 (t, $J = 7.3$ Hz, 2H), 2.61 (d, $J = 10.1$ Hz, 4H), 2.49 - 2.43 (m, 2H), 2.32 (s, 3H), 1.56 (p, $J = 7.4$ Hz, 2H), 1.46 (s, 18H), 1.43 - 1.32 (m, 5H), and 1.25 (s, 26H).

¹³C NMR (126 MHz, CDCl₃) δ (ppm) = 196.00, 155.70, 155.55, 155.39, 79.33, 57.03, 56.89, 54.09, 54.04, 53.64, 50.65, 50.58, 50.36, 50.17, 50.02, 49.73, 31.49, 30.42, 30.61, 30.18, 29.68, 29.62, 29.56, 29.49, 29.46, 29.14, 29.10, 28.81, 28.57, 28.55, 28.09,

27.93, 27.73, 27.55, 27.46, and 27.40.

HRMS (ESI-MS) m/z : $[M+H]^+$ Calcd. 656.5031; Found: 656.5029.

1.5. Synthesis of **4**



Scheme S5. The synthesis route of **4**.

Compound **3** was dissolved in 5 mL of methanol hydrochloric acid mixed solvent (with 1:1 ratio by volume). The solution was stirred at 60 °C for 6 h. The solvent was removed by using rotary evaporation under a vacuum to afford pure compound **4** (**4a-4c**).

4a: $^1\text{H NMR}$ (500 MHz, CD_3OD) $\delta(\text{ppm}) = 3.59$ (s, 4H), 3.35 (d, $J = 5.7$ Hz, 4H), 3.13 (t, $J = 5.7$ Hz, 4H), 2.90 - 2.84 (m, 2H), 2.52 (t, $J = 7.7$ Hz, 2H), 1.71 - 1.59 (m, 5H), and 1.49 - 1.30 (m, 8H).

HRMS (ESI-MS) m/z : $[M+H]^+$ Calcd. 260.2155; Found: 260.2151.

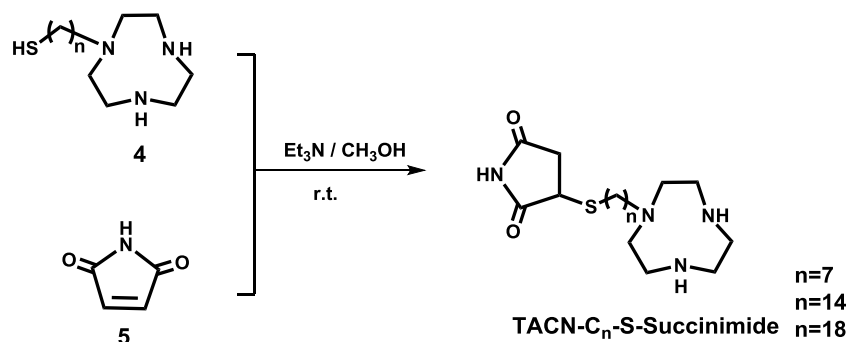
4b: $^1\text{H NMR}$ (500 MHz, CD_3OD) $\delta(\text{ppm}) = 3.58$ (s, 4H), 3.35 (d, $J = 5.8$ Hz, 4H), 3.12 (t, $J = 5.8$ Hz, 4H), 2.90 - 2.85 (m, 2H), 2.53 - 2.49 (m, 2H), 1.69 - 1.58 (m, 4H), 1.44 - 1.39 (m, 3H), and 1.31 (s, 20H).

HRMS (ESI-MS) m/z : $[M+H]^+$ Calcd. 357.2319; Found: 357.2319.

4c: $^1\text{H NMR}$ (500 MHz, CD_3OD) $\delta(\text{ppm}) = 3.58$ (s, 4H), 3.35 (d, $J = 5.8$ Hz, 4H), 3.12 (t, $J = 5.8$ Hz, 4H), 2.89 - 2.85 (m, 2H), 2.51 (t, $J = 7.2$ Hz, 2H), 1.67 (dd, $J = 16.1, 7.5$ Hz, 2H), 1.61 (d, $J = 15.0$ Hz, 2H), 1.44 - 1.38 (m, 3H), and 1.31 (s, 28H).

HRMS (ESI-MS) m/z : $[M+H]^+$ Calcd. 414.3876; Found: 414.3875.

1.6. Synthesis of TACN- C_n -S-Succinimide ($n=7, 14, \text{ and } 18$)



Scheme S6. The synthesis route of **TACN-C_n-S-Succinimide (n=7, 14, and 18)**.^{S1}

3 equiv of triethylamine and 1 equiv of Maleimide were added to 5 mL methanol solution containing 1 equiv of compound **4**. The mixed solution was stirred at room temperature for 4 h. The solvent was removed by using rotary evaporation under a vacuum to afford the crude product **TACN-C_n-S-Succinimide (n=7, 14, and 18)**. The crude product was purified by using silica gel column chromatography (eluent: V_{PE}/V_{EA} = 5/1) to obtain a pure compound **TACN-C_n-S-Succinimide (n=7, 14, and 18)**.

TACN-C₇-S-Succinimide: ¹H NMR (500 MHz, CD₃OD) δ(ppm) = 3.87 (dd, *J* = 9.0, 3.8 Hz, 1H), 3.67 (d, *J* = 3.5 Hz, 2H), 3.55 (s, 4H), 3.30 (t, *J* = 5.8 Hz, 4H), 3.03 (t, *J* = 5.8 Hz, 4H), 2.89 - 2.83 (m, 1H), 2.79 - 2.71 (m, 3H), 2.49 (dd, *J* = 18.6, 3.8 Hz, 1H), 1.71 - 1.54 (m, 5H), 1.43 (dq, *J* = 21.8, 8.0, 7.2 Hz, 5H), and 1.31 (s, 8H).

HRMS (ESI-MS) m/z: [M+H]⁺ Calcd. 357.2319; Found: 357.2319.

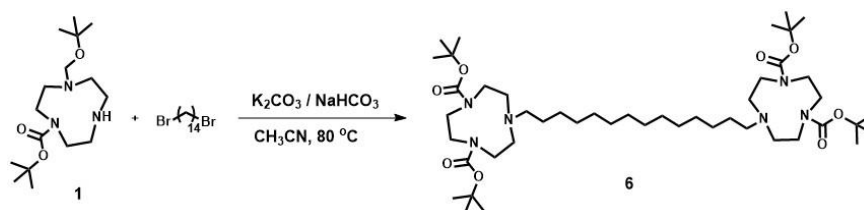
TACN-C₁₄-S-Succinimide: ¹H NMR (500 MHz, CD₃OD) δ(ppm) = 3.87 (dd, *J* = 9.1, 3.8 Hz, 1H), 3.52 (s, 4H), 3.30 (s, 4H), 3.22 (dd, *J* = 18.6, 9.1 Hz, 2H), 3.03 (t, *J* = 5.9 Hz, 4H), 2.89 - 2.82 (m, 1H), 2.80 - 2.71 (m, 3H), 2.49 (dd, *J* = 18.6, 3.8 Hz, 1H), 1.73 - 1.52 (m, 5H), 1.47 - 1.40 (m, 2H), and 1.33 (s, 20H).

HRMS (ESI-MS) m/z: [M+H]⁺ Calcd. 455.3414; Found: 455.3418.

TACN-C₁₈-S-Succinimide: ¹H NMR (500 MHz, CD₃OD) δ(ppm) = 3.79 (dd, *J* = 9.0, 3.8 Hz, 1H), 3.49 (s, 4H), 3.27 - 3.16 (m, 5H), 3.00 (t, *J* = 5.8 Hz, 4H), 2.86 - 2.80 (m, 1H), 2.76 - 2.68 (m, 3H), 2.51 (dd, *J* = 18.8, 3.8 Hz, 1H), 1.63 (dq, *J* = 14.6, 7.3 Hz, 2H), 1.52 (q, *J* = 7.7, 7.2 Hz, 2H), 1.44 - 1.34 (m, 3H), and 1.26 (s, 28H).

HRMS (ESI-MS) m/z: [M+H]⁺ Calcd. 511.4040; Found: 511.4041.

1.8. Synthesis of 6



Scheme S7. The synthesis route of **6**.^{S2}

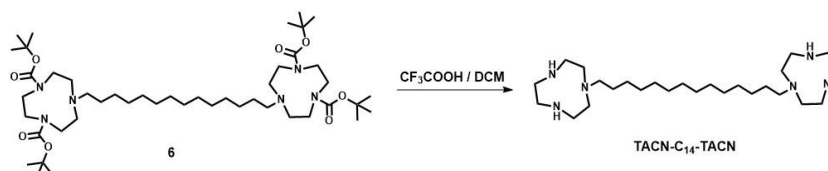
3 equiv of K_2CO_3 , 3 equiv of $NaHCO_3$, and 106.8 mg (0.2 mmol) of 1,14-dibromotetradecane were added to 10 mL acetonitrile solution containing 98.7 mg (0.3 mmol) of compound **1**. The mixed solution was stirred overnight at 80 °C. After the organic phase was extracted and dried by anhydrous $MgSO_4$. The solvent was removed by using rotary evaporation under a vacuum, and the crude product was purified by using silica gel column chromatography (eluent: $V_{PE}/V_{EA} = 10/1$) to obtain 0.146 g of an oil-like pure compound **6**.

1H NMR (500 MHz, $CDCl_3$) δ (ppm) = 3.43 (d, $J = 22.0$ Hz, 8H), 3.22 (d, $J = 22.9$ Hz, 8H), 2.59 (d, $J = 14.6$ Hz, 8H), 2.44 (dq, $J = 8.5, 4.5$ Hz, 4H), 1.43 (s, 36H), 1.38 (d, $J = 12.7$ Hz, 4H), and 1.22 (s, 20H).

^{13}C NMR (126 MHz, $CDCl_3$) δ (ppm) = 155.66, 155.52, 155.36, 79.32, 79.28, 79.25, 56.93, 56.81, 53.96, 53.92, 53.55, 50.59, 50.54, 50.30, 50.12, 49.89, 49.66, 29.65, 28.55, 28.52, 28.05, 27.88, 27.67, 27.52, 27.43, and 27.37.

HRMS (ESI-MS) m/z : $[M+H]^+$ Calcd. 853.6737; Found: 853.6740.

1.9. Synthesis of TACN-C₁₄-TACN



Scheme S8. The synthesis route of **TACN-C₁₄-TACN**.

Compound **7** was dissolved in 5 mL of dichloromethane -trifluoroacetic acid

mixed solvent (with 1:1 ratio by volume). The solution was stirred at room temperature for 4 h. The solvent was removed by using rotary evaporation under a vacuum to obtain pure compound **TACN-C14-TACN**.

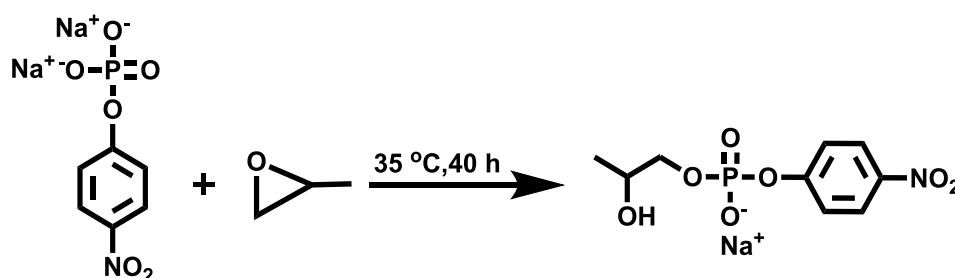
¹H NMR (500 MHz, CD₃OD) δ(ppm) = 3.54 (s, 8H), 3.29 (t, *J* = 5.9 Hz, 8H), 3.03 (t, *J* = 5.8 Hz, 8H), 2.78 - 2.72 (m, 4H), 1.58 (p, *J* = 7.6 Hz, 4H), and 1.31 (s, 20H).

¹³C NMR (126 MHz, CD₃OD) δ(ppm) = 56.43, 54.78, 43.06, 43.03, 41.71, 41.27, 33.04, 32.33, 32.10, 31.08, 30.91, 29.36, 29.34, 29.30, 29.24, 29.18, 28.44, 27.76, 26.51, 26.34, 26.23, 24.36, 22.42, 21.98, 15.56, and 15.16.

HRMS (ESI-MS) *m/z*: [M+H]⁺ Calcd. 453.4639; Found: 453.4632.

2.1. Synthesis and characterization of HPNP

2.1.1. Synthesis of HPNP



Scheme S9. The synthesis route of **HPNP**.^{S3}

¹H NMR (500 MHz, D₂O) δ(ppm) = 8.15 (d, *J* = 9.0 Hz, 2H), 7.24 (d, *J* = 9.4 Hz, 2H), 3.94 - 3.79 (m, 2H), 3.73 - 3.66 (m, 1H), and 1.03 (d, *J* = 7.5 Hz, 3H).

¹³C NMR (126 MHz, D₂O) δ(ppm) = 148.88, 125.79, 120.89, 120.36, 70.98, 67.54, and 17.57.

³¹P NMR (202 MHz, D₂O) δ(ppm) = -4.89.

HRMS (ESI-MS) *m/z*: [M+H]⁺ Calcd. 276.0276; Found: 276.0279.

Computational Details:

Density functional theory (DFT) calculations were carried out using Gaussian 16 programs^{S4} and ORCA 5.0.3^{S5-S8} in this work. All geometric optimizations have been carried out by density functional theory using the B3LYP hybrid functional^{S9} with Grimme's dispersion correction of D3 version (Becke-Johnson damping)^{S10}. The

standard 6-31G(d,p) basis set^{S11-S13} for H, C, N, O and P was used. For the Zn and Ag atoms, the SDD basis set and its corresponding effective core potential^{S14-S15} was used. Harmonic vibration frequency calculations were performed for all stationary points to confirm them as a local minima or transition state. The intrinsic reaction coordinate (IRC) scheme^{S16-S17} was applied for the calculations of the reaction coordinates to confirm whether or not the transition states were directly connected to the reactants and products. The single-point energy (SP) calculations were performed on the optimized geometries at PWPB95-D3(BJ)/def2-TZVPP theoretical level^{S18-S21}. Approximate solvent (water molecules) effects were taken into consideration based on the continuum solvation model in optimization^{S22} and SP^{S23} calculations. The SP calculations were carried out by the ORCA 5.0.3^{S5-S8}.

References:

- (S1) Q. N. Lin, C. Y. Bao, S. Y. Cheng, Y. L. Yang, W. Ji, L. Y. Zhu, *Journal of the American Chemical Society*. 2012, **134**, 5052-5055.
- (S2) J. Czescik, Y. C. Lyu, S. Neuberger, P. Scrimin, F. Mancin, *Journal of the American Chemical Society*. 2020, **142**, 6837-6841.
- (S3) Y. J. Cao, M. X. Yao, L. J. Prins, R. X. Ji, N. Liu, X. Y. Sun, Y. B. Jiang, J. S. Shen, *Chemistry-A European Journal*. 2021, **27**, 7646-7650.
- (S4) Gaussian 16, Revision C.01, M. J. Frisch, G. W. Trucks, H. B. Schlegel, G. E. Scuseria, M. A. Robb, J. R. Cheeseman, G. Scalmani, V. Barone, G. A. Petersson, H. Nakatsuji, X. Li, M. Caricato, A. V. Marenich, J. Bloino, B. G. Janesko, R. Gomperts, B. Mennucci, H. P. Hratchian, J. V. Ortiz, A. F. Izmaylov, J. L. Sonnenberg, D. Williams-Young, F. Ding, F. Lipparini, F. Egidi, J. Goings, B. Peng, A. Petrone, T. Henderson, D. Ranasinghe, V. G. Zakrzewski, J. Gao, N. Rega, G. Zheng, W. Liang, M. Hada, M. Ehara, K. Toyota, R. Fukuda, J. Hasegawa, M. Ishida, T. Nakajima, Y. Honda, O. Kitao, H. Nakai, T. Vreven, K. Throssell, J. A. Jr. Montgomery, J. E. Peralta, F. Ogliaro, M. J. Bearpark, J. J. Heyd, E. N. Brothers, K. N. Kudin, V. N. Staroverov, T. A. Keith, R. Kobayashi, J. Normand, K. Raghavachari, A. P. Rendell, J. C. Burant, S. S. Iyengar, J. Tomasi, M. Cossi, J. M. Millam, M. Klene, C. Adamo, R. Cammi, J. W.

Ochterski, R. L. Martin, K. Morokuma, O. Farkas, J. B. Foresman, Fox, D. J. Gaussian, Inc., Wallingford CT, 2016.

(S5) F. Neese, *Wiley Interdisciplinary Reviews-computational Molecular Science*. 2012, **2**, 73-78.

(S6) F. Neese, *Wiley Interdisciplinary Reviews-computational Molecular Science*. 2017, **8**, e1327.

(S7) F. Neese, F. Wennmohs, U. Becker, C. Riplinger, *The Journal of Chemical Physics*. 2020, **152**, 224108.

(S8) F. Neese, *Wiley Interdisciplinary Reviews-computational Molecular Science*. 2022, **12**, e1606.

(S9) P. J. Stephens, F. J. Devlin, C. F. Chabalowski, Frisch, M. J. *The Journal of Chemical Physics*. 1994, **98**, 11623-11627.

(S10) S. Grimme, S. Ehrlich, L. Goerigk, *Journal of Computational Chemistry*. 2011, **32**, 1456-1465.

(S11) W. J. Hehre, R. Ditchfield, Pople, *The Journal of Chemical Physics*. 1972, **56**, 2257-2261.

(S12) M. M. Francl, W. J. Pietro, W. J. Hehre, J. S. Binkley, M. S. Gordon, D.J. DeFrees, J. A. Pople, *The Journal of Chemical Physics*. 1982, **77**, 3654-3665.

(S13) T. Clark, J. P. v. R. Chandrasekhar Schleyer, *Journal Of Computational Chemistry*. 1983, **4**, 294-301.

(S14) M. Dolg, U. Wedig, H. Stoll, H. Preuss, *The Journal of Chemical Physics*. 1987, **86**, 866-872.

(S15) D. Andrae, U. H. äüßermann, M. Dolg, H. H. Stoll Preuß, *Theoretica chimica acta*. 1990, **77**, 123-141.

(S16) K. Fukui, *The Journal of Chemical Physics*. 1970, **74**, 4161-4163.

(S17) K. Fukui, *Accounts of Chemical Research*. 1981, **14**, 363-368.

(S18) L. Goerigk, S. Grimme, *Journal of Chemical Theory and Computation*. 2011, **7**, 291-309.

(S19) S. Grimme, S. Ehrlich, L. Goerigk, *Journal of Computational Chemistry*. 2011,

32, 1456-1465.

(S20) F. Weigend, R. Ahlrichs, *Physical Chemistry Chemical Physics*. 2005, **7**, 3297-3305.

(S21) F. Weigend, *Physical Chemistry Chemical Physics*. 2006, **8**, 1057-1065.

(S22) J. Tomasi, B. Mennucci, R. Cammi, *Chemical Reviews*. 2005, **105**, 2999-3094.

(S23) A. V. Marenich, C. J. Cramer, D. G. Truhlar, *The Journal of Physical Chemistry B*. 2009, **113**, 6378-6396.

3. Supplementary experimental results

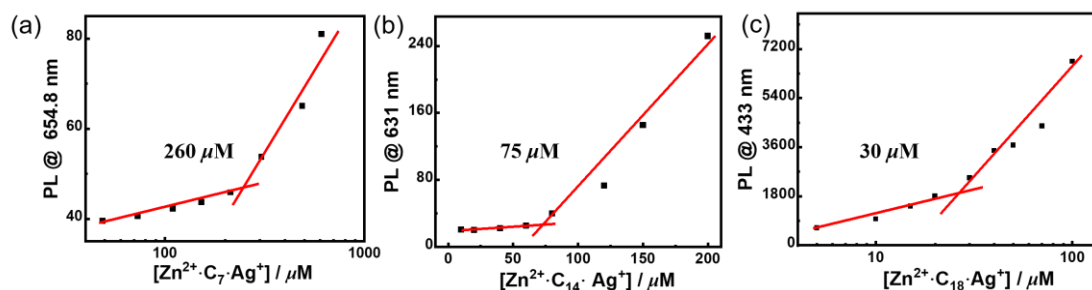


Figure S1. (a)-(c) are the relationships between $[\text{Zn}^{2+} \text{C}_n \text{Ag}^+]$ and PL intensity at maximum emission wavelength, respectively ($n = 7$ for b, 14 for c, and 18 for d), measured by using NR (a and b) or DPH (c) as the fluorescent probe. The intersection is indicative of corresponding CAC value. Experimental conditions: $[\text{TACN-C}_7\text{-S-Succinimide}] = 350 \mu\text{M}$; $[\text{TACN-C}_{18}\text{-S-Succinimide}] = 150 \mu\text{M}$; $[\text{Zn}^{2+}] = 350/150 \mu\text{M}$; $[\text{Ag}^+] = 350/150 \mu\text{M}$.

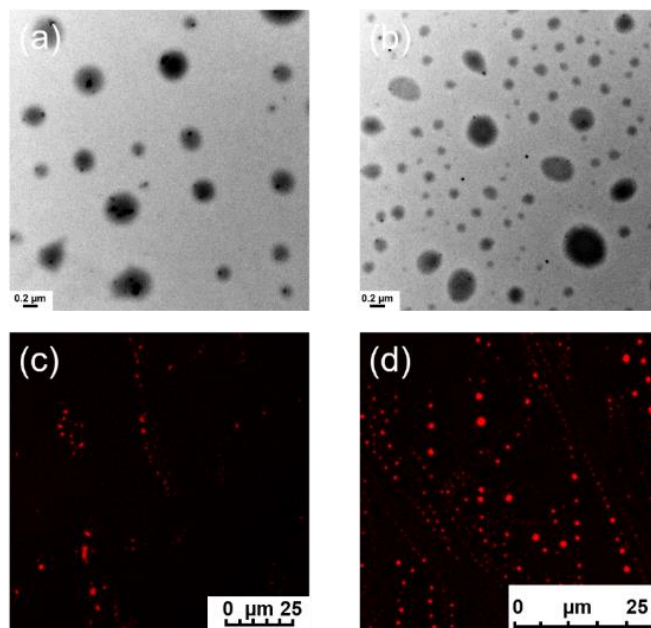


Figure S2. TEM (a, b) and LSCM (c, d) images of $\text{Zn}^{2+} \cdot \text{TACN-C}_7\text{-S-Succinimide} \cdot \text{Ag}^+$ (a, c) and $\text{Zn}^{2+} \cdot \text{TACN-C}_{18}\text{-S-Succinimide} \cdot \text{Ag}^+$ (b, d). Experimental conditions: $[\text{TACN-C}_7\text{-S-Succinimide}] = 350 \mu\text{M}$; $[\text{TACN-C}_{18}\text{-S-Succinimide}] = 150 \mu\text{M}$; $[\text{Zn}^{2+}] = 350/150 \mu\text{M}$; $[\text{Ag}^+] = 350/150 \mu\text{M}$.

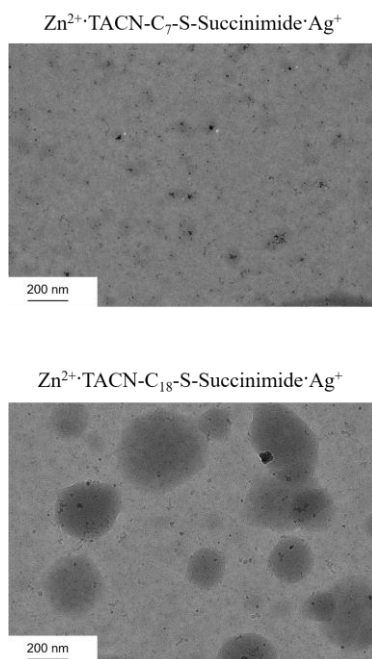


Figure S3. Cryo-TEM image of vesicles with $[\text{Zn}^{2+} \cdot \text{TACN-C}_7\text{-S-Succinimide} \cdot \text{Ag}^+] = 350 \mu\text{M}$, $[\text{Zn}^{2+} \cdot \text{TACN-C}_{18}\text{-S-Succinimide} \cdot \text{Ag}^+] = 150 \mu\text{M}$. Scale bar, 200 nm.

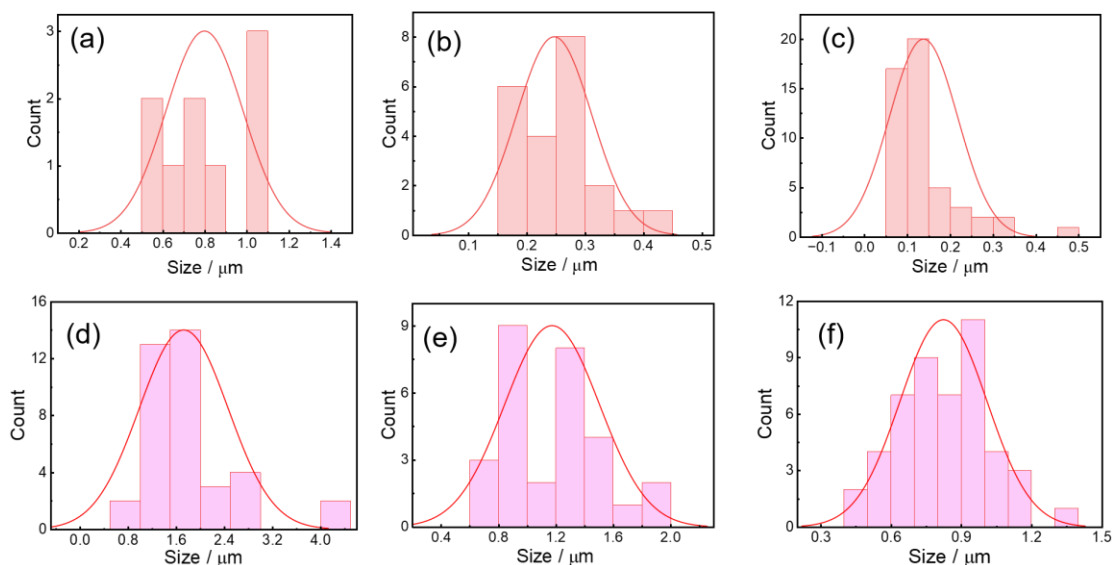


Figure S4. The size distribution graphs, calculated from TEM experiments, of TACN-C₇-S-Succinimide (a), TACN-C₁₄-S-Succinimide (b), and TACN-C₁₈-S-Succinimide (c), and from LSCM experiments, of TACN-C₇-S-Succinimide (d), TACN-C₁₄-S-Succinimide (e), and TACN-C₁₈-S-Succinimide (f).

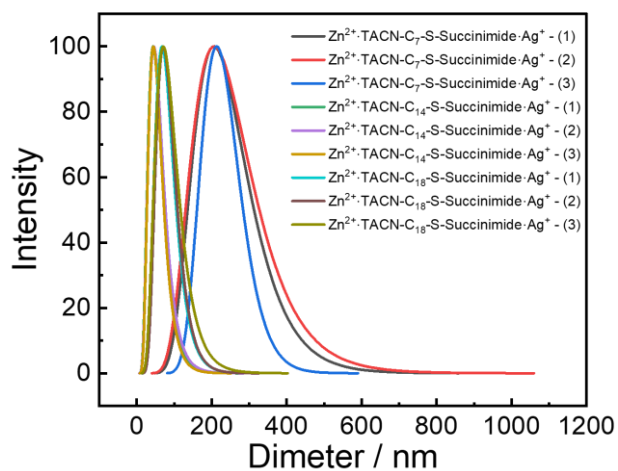


Figure S5. Hydrodynamic diameter of $\text{Zn}^{2+}\cdot\text{TACN-C}_7\text{-S-Succinimide}\cdot\text{Ag}^+$, $\text{Zn}^{2+}\cdot\text{TACN-C}_{14}\text{-S-Succinimide}\cdot\text{Ag}^+$ and $\text{Zn}^{2+}\cdot\text{TACN-C}_{18}\text{-S-Succinimide}\cdot\text{Ag}^+$, measured by DLS. Each sample was repeatedly measured three times, marked “1”, “2”, and “3”, respectively.

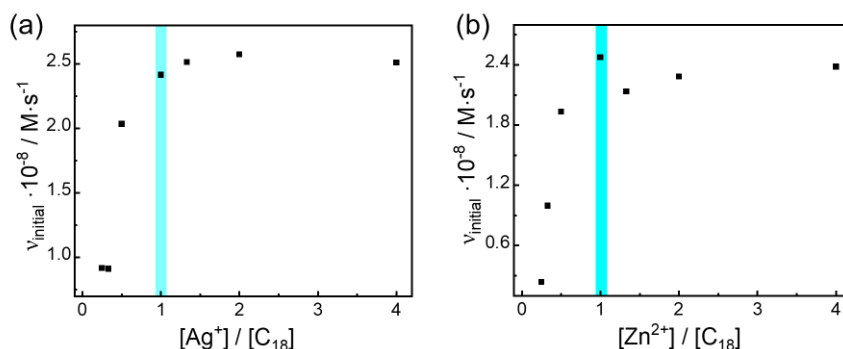


Figure S6. (a) The relationship between $[Ag^+] / [C_{18}]$ and initial rate to indicate the turning points of the molar ratio of TACN- C_{18} -S-Succinimide to Ag^+ (both TACN- C_{18} -S-Succinimide concentration and Zn^{2+} ions concentration were fixed as $80 \mu M$). (b) The relationship between $[Zn^{2+}] / [C_{18}]$ and initial rate to indicate the turning point of the molar ratio of TACN- C_{18} -S-Succinimide to Zn^{2+} (both TACN- C_{18} -S-Succinimide concentration and Ag^+ ions concentration were fixed as $80 \mu M$).

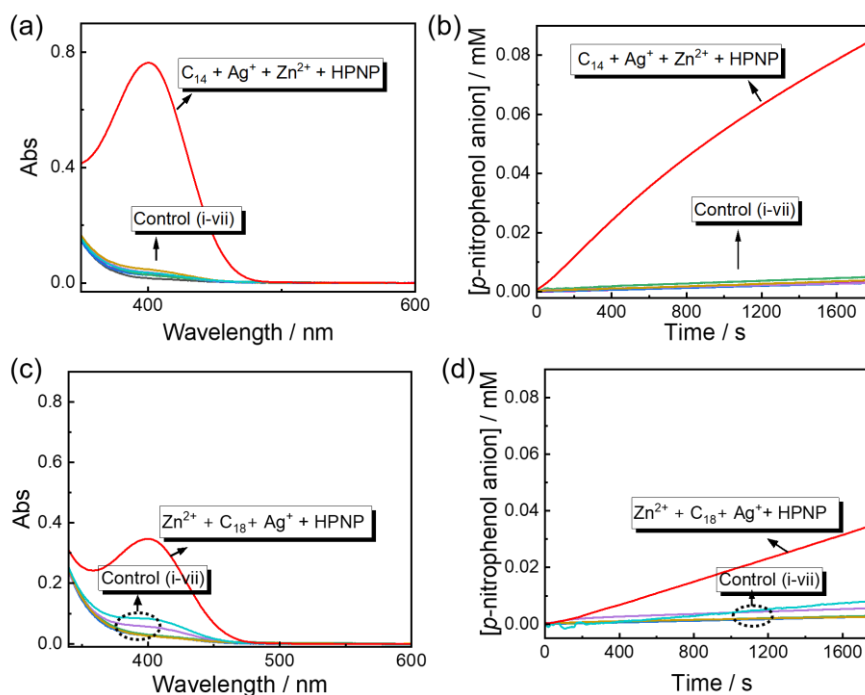


Figure S7. UV-vis absorption spectra (a: C_{14} , c: C_{18}) and incubation time-dependent p -nitrophenol anion concentration change curves (b: C_{14} , d: C_{18}) of $150 \mu M$ HPNP solution containing $100 \mu M$ TACN- C_n -S-Succinimide ($n=14, 18$), $100 \mu M$ Zn^{2+} , and $100 \mu M$ Ag^+ (red line), of other control systems ($150 \mu M$ HPNP solution containing i: $100 \mu M$ Ag^+ ; ii: $100 \mu M$ Zn^{2+} ; iii: $100 \mu M$ Zn^{2+} plus $100 \mu M$ Ag^+ ; iv: $100 \mu M$ TACN- C_n -S-Succinimide ($n=14, 18$) plus $100 \mu M$ Ag^+ ; v: $100 \mu M$ TACN- C_n -S-Succinimide ($n=14,$

18) plus 100 μM Zn^{2+} ; vi: 100 μM TACN- C_n -S-Succinimide($n=14, 18$) plus 200 μM Ag^+ , and vii: 100 μM TACN- C_n -S-Succinimide($n=14, 18$) plus 200 μM Zn^{2+} , respectively). 10 mM HEPES buffer solution of pH 7.5, 37 $^\circ\text{C}$ (for a and c, kept at 37 $^\circ\text{C}$ for 30 min to measure their spectra).

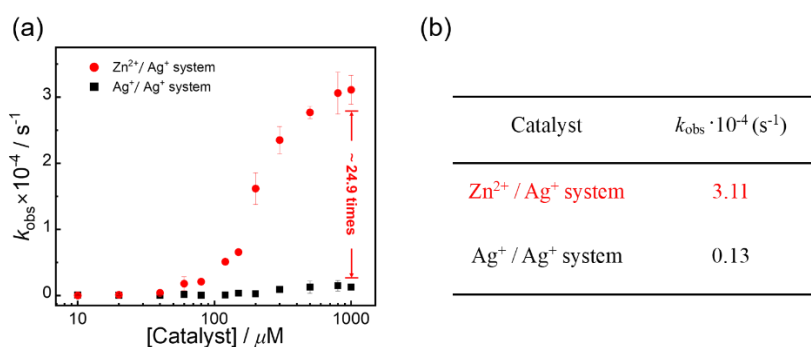


Figure S8. (a) The comparison between the relationships between k_{obs} and [catalyst] (red squares represent $\text{Zn}^{2+} \cdot \text{TACN-C}_{14}\text{-S-Succinimide} \cdot \text{Ag}^+$, and black squares represent $\text{Ag}^+ \cdot \text{TACN-C}_{14}\text{-S-Succinimide} \cdot \text{Ag}^+$). HPNP concentration was fixed as 100 μM , and temperature was 37 $^\circ\text{C}$. (b) The k_{obs} values of TACN- C_{14} -S-Succinimide with $\text{Zn}^{2+} / \text{Ag}^+$ system and $\text{Ag}^+ / \text{Ag}^+$ system ($[\text{catalyst}] = 1000 \mu\text{M}$).

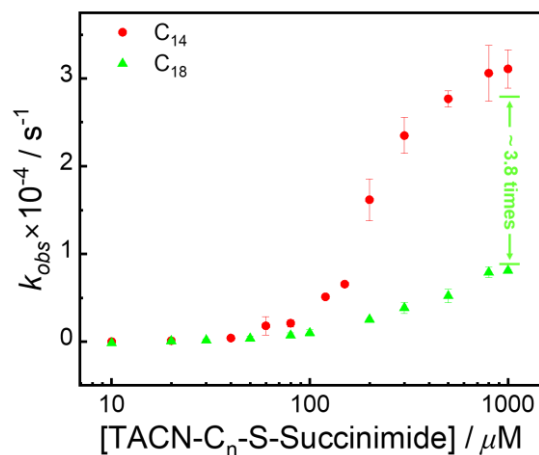


Figure S9. The comparison between the relationships between k_{obs} and [catalyst] (Red squares represent $\text{Zn}^{2+}\cdot\text{TACN-C}_{14}\text{-S-Succinimide}\cdot\text{Ag}^+$, and green triangles represent $\text{Zn}^{2+}\cdot\text{TACN-C}_{18}\text{-S-Succinimide}\cdot\text{Ag}^+$). HPNP concentration was fixed as $100\ \mu\text{M}$, and temperature was $37\ ^\circ\text{C}$.

Table S1. V_{max} and K_{M} values obtained from fitting Michaelis-Menten equation curves in $\text{Zn}^{2+}\cdot\text{TACN-C}_{14}\text{-S-Succinimide}\cdot\text{Ag}^+$ and $\text{Zn}^{2+}\cdot\text{TACN-C}_{18}\text{-S-Succinimide}\cdot\text{Ag}^+$ assemblies (error values were obtained from three parallel measurements).

	$V_{\text{max}}\ (\text{M}\ \text{s}^{-1})$	$K_{\text{M}}\ (\text{mM})$
$\text{Zn}^{2+}\cdot\text{TACN-C}_{14}\text{-S-Succinimide}\cdot\text{Ag}^+$	$(2.28 \pm 0.31) \times 10^{-7}$	0.56 ± 0.09
$\text{Zn}^{2+}\cdot\text{TACN-C}_{18}\text{-S-Succinimide}\cdot\text{Ag}^+$	$(3.51 \pm 0.45) \times 10^{-7}$	1.30 ± 0.29

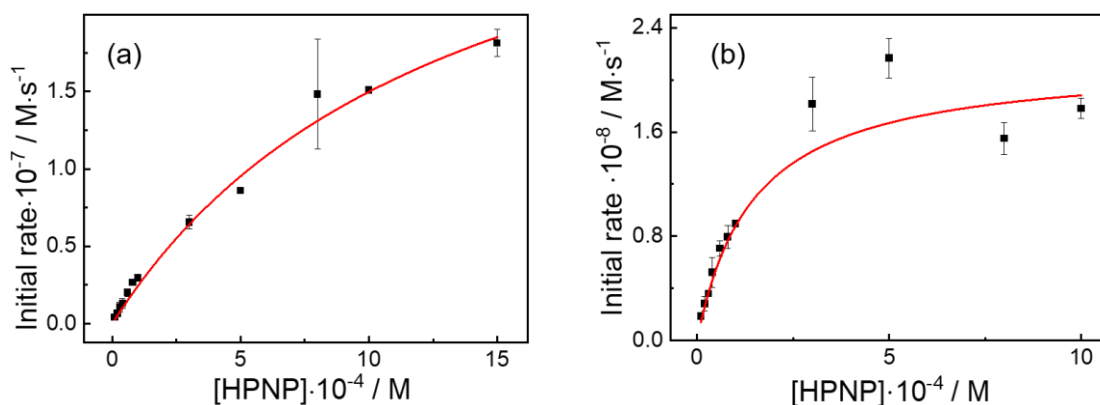


Figure S10. The initial rate of $\text{Zn}^{2+}\cdot\text{TACN}\text{-C}_{18}\text{-S}\text{-Succinimide}\cdot\text{Ag}^+$ (a) or $\text{Zn}^{2+}\cdot\text{TACN}\text{-C}_{18}\text{-S}\text{-Succinimide}\cdot\text{Zn}^{2+}$ (b) as a function of substrate HPNP concentration, fitted by the Michaelis-Menten equation (red lines). Experimental conditions: $[\text{TACN}\text{-C}_{18}\text{-S}\text{-Succinimide}] = 100 \mu\text{M}$; $[\text{Zn}^{2+}] = 100 \mu\text{M}$; $[\text{Ag}^+] = 100 \mu\text{M}$; 10 mM HEPES buffer solution of pH 7.5; temperature was set as 37 °C. The error bars were obtained from three parallel measurements.

Table S2. Fitted V_{\max} and K_M values of the hydrolysis reaction of HPNP catalyzed by TACN-C₁₈-S-Succinimide ($\text{Zn}^{2+}/\text{Ag}^+$ and $\text{Zn}^{2+}/\text{Zn}^{2+}$) systems, respectively.^a

No.	Catalyst	V_{\max} (M s^{-1})	K_M (mM)
1	$\text{Zn}^{2+}\cdot\text{TACN}\text{-C}_{18}\text{-S}\text{-Succinimide}\cdot\text{Ag}^+$	$(3.51 \pm 0.45) \times 10^{-7}$	1.30 ± 0.29
2	$\text{Zn}^{2+}\cdot\text{TACN}\text{-C}_{18}\text{-S}\text{-Succinimide}\cdot\text{Zn}^{2+}$	$(2.15 \pm 0.15) \times 10^{-9}$	0.15 ± 0.01

a. Experimental conditions: 10 mM HEPES buffer solution of pH 7.5; temperature was set as 37 °C. $[\text{TACN}\text{-C}_{18}\text{-S}\text{-Succinimide}] = 100 \mu\text{M}$. $[\text{Zn}^{2+}] = 100$ (1) / 200 (2) μM . $[\text{Ag}^+] = 100$ (1) μM .

Table S3. Summary of CAC values (μM) of Zn^{2+} , TACN- C_n -S-Succinimide ($n=7$ (No. 1), 14 (No.2), and 18 (No.3)), and other tested metal ions mixed systems with an equimolar ratio (1:1:1), measured by a fluorescence probe method.

No.	Ag^+	Cu^{2+}	Pb^{2+}	Fe^{3+}	Cd^{2+}	Ni^{2+}	Mg^{2+}	Ca^{2+}	Al^{3+}	Hg^{2+}
1	260	325	60	285	150	325	160	180	180	285
2	75	76	54	110	70	74	75	62	68	80
3	30	58	43	78	50	57	55	62	67	54

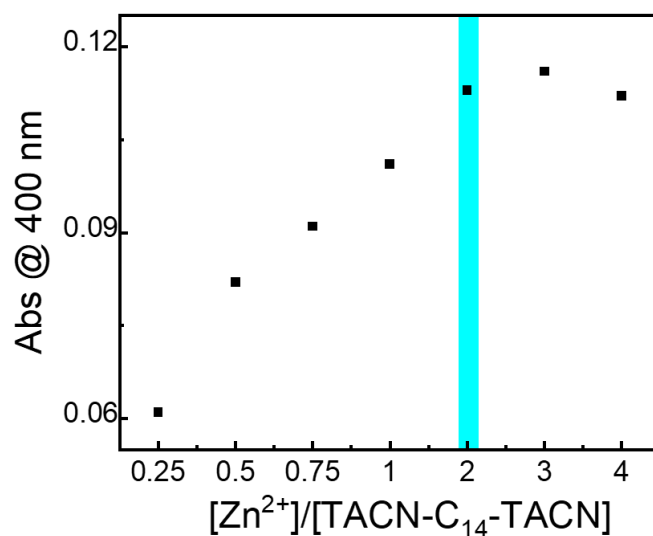


Figure S11. The relationship between $[\text{Zn}^{2+}]/[\text{TACN-C}_{14}\text{-TACN}]$ and Abs@400 nm to indicate the turning point of the molar ratio of TACN- C_{14} -TACN to Zn^{2+} . Experimental conditions: 10 mM HEPES buffer, pH 7.5; $T=37\text{ }^\circ\text{C}$; $[\text{HPNP}] = 150\text{ }\mu\text{M}$; $[\text{TACN-C}_{14}\text{-TACN}] = 100\text{ }\mu\text{M}$; the spectral measurements were conducted after the mixed solution was kept at $37\text{ }^\circ\text{C}$ for 30 min.

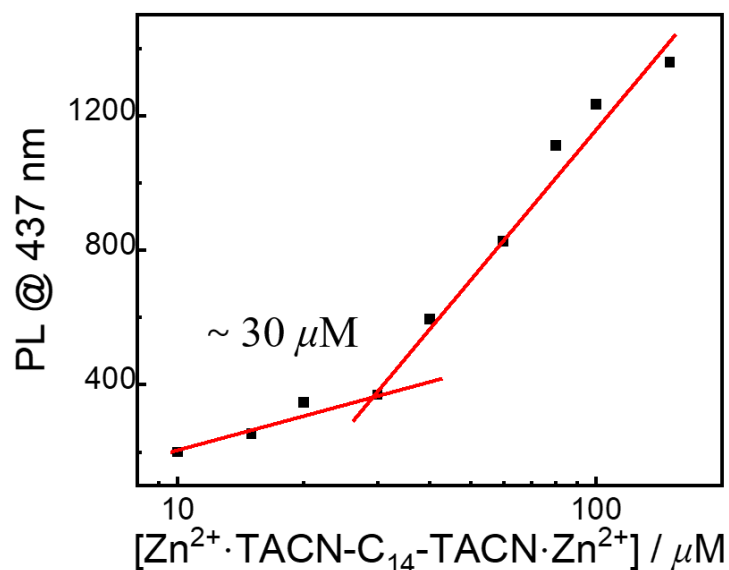


Figure S12. The relationship between $[\text{Zn}^{2+} \cdot \text{TACN-C}_{14}\text{-TACN} \cdot \text{Zn}^{2+}]$ and PL intensity at maximum emission wavelength, measured by using DPH as the fluorescent probe. The intersection is indicative of corresponding CAC value. Experimental conditions: 10 mM HEPES buffer of pH 7.5; $[\text{DPH}] = 10 \mu\text{M}$; $T = 37 \text{ }^\circ\text{C}$; excitation wavelength = 360 nm; slit_{ex} / slit_{em} = 2.5 nm / 5 nm.

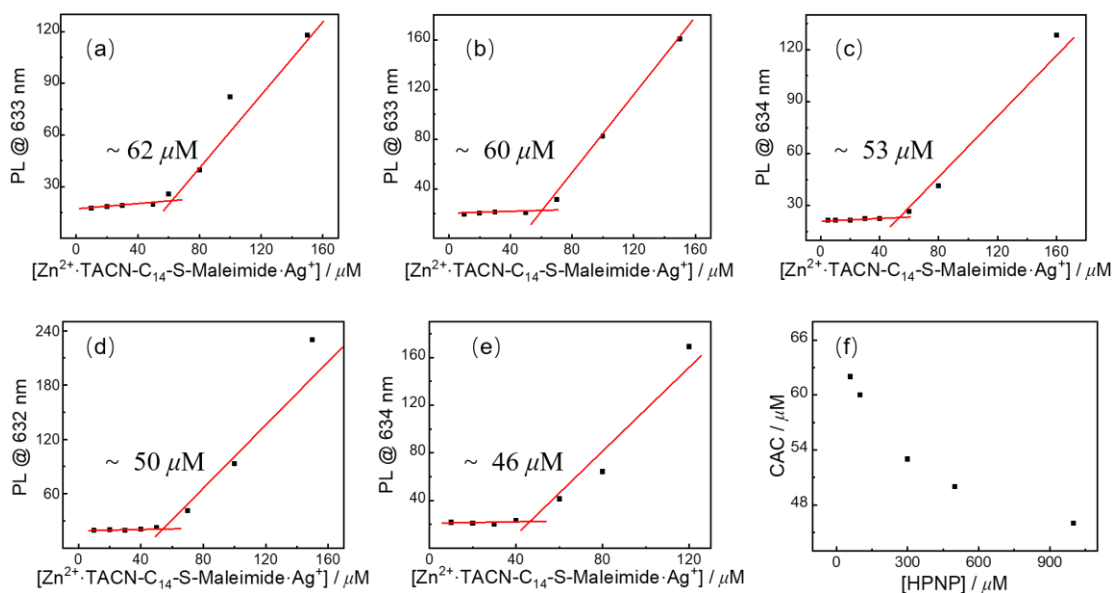


Figure S13. (a-e) are the relationships between $[\text{Zn}^{2+} \cdot \text{TACN-C}_{14}\text{-S-Succinimide} \cdot \text{Ag}^+]$ and PL intensity at maximum emission wavelength (a, 60 μM ; b, 100 μM ; c, 300 μM ; d, 500 μM ; e, 1000 μM HPNP), measured by NR as the fluorescent probe, and the relationship between CAC value and HPNP concentration in $\text{Zn}^{2+} \cdot \text{TACN-C}_{14}\text{-S-}$

Succinimide Ag^+ case (f). The intersection (a-e) is indicative of corresponding CAC value. Experimental conditions: 10 mM HEPES buffer of pH 7.5; $[\text{NR}] = 10 \mu\text{M}$; $T = 37 \text{ }^\circ\text{C}$; $\lambda_{\text{ex}} = 564 \text{ nm}$; $\text{slit}_{\text{ex}} / \text{slit}_{\text{em}} = 2.5 \text{ nm} / 5 \text{ nm}$.

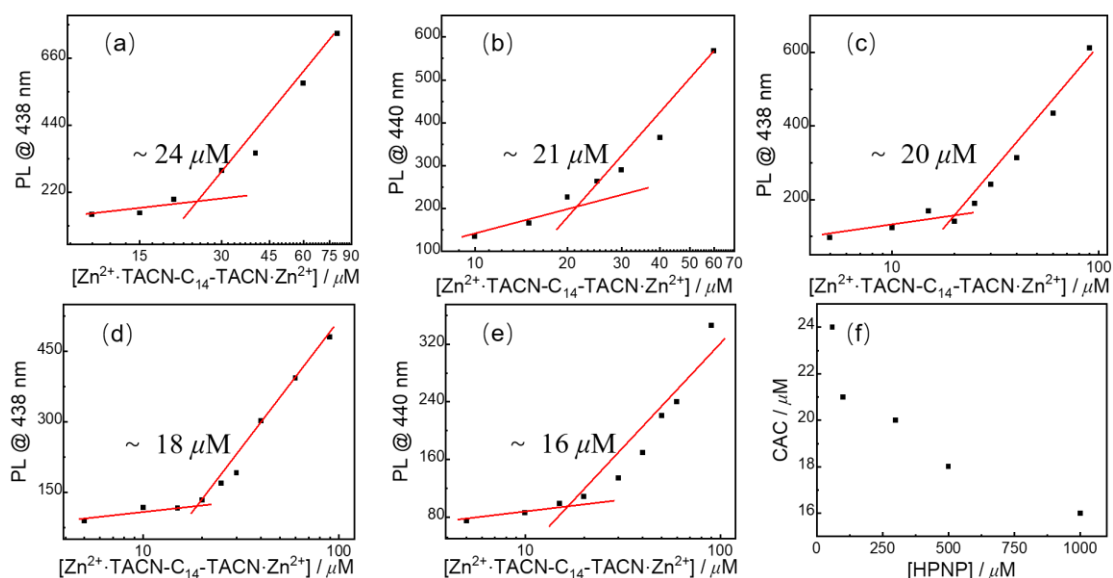


Figure S14. (a-e) are the relationships between $[\text{Zn}^{2+} \cdot \text{TACN-C}_{14}\text{-TACN} \cdot \text{Zn}^{2+}]$ and PL intensity at maximum emission wavelength (a, $60 \mu\text{M}$; b, $100 \mu\text{M}$; c, $300 \mu\text{M}$; d, $500 \mu\text{M}$; e, $1000 \mu\text{M}$ HPNP), measured by DPH as the fluorescent probe, and the relationship between CAC value and HPNP concentration in $\text{Zn}^{2+} \cdot \text{TACN-C}_{14}\text{-TACN} \cdot \text{Zn}^{2+}$ case (f). The intersection (a-e) is indicative of corresponding CAC value. Experimental conditions: 10 mM HEPES buffer of pH 7.5; $[\text{DPH}] = 10 \mu\text{M}$; $T = 37 \text{ }^\circ\text{C}$; $\lambda_{\text{ex}} = 360 \text{ nm}$; $\text{slit}_{\text{ex}} / \text{slit}_{\text{em}} = 2.5 \text{ nm} / 5 \text{ nm}$.

4. ^1H NMR, ^{13}C NMR, and MS characterization of synthesized compounds

4.1 Characterization of TACN- C_n -S-Succinimide ($n=7, 14,$ and 18), control TACN- C_{14} -TACN, and substrate HPNP

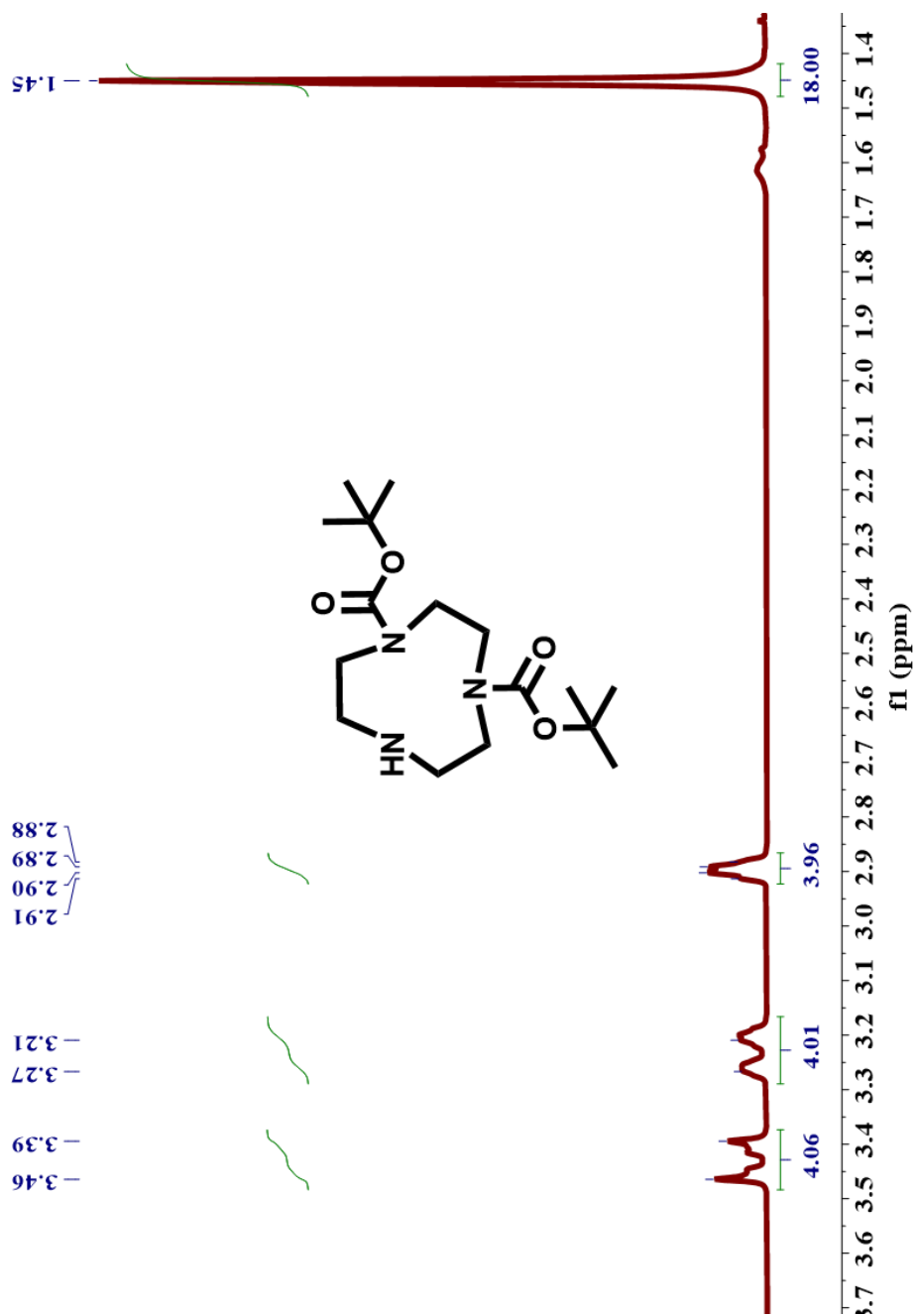


Figure S15. ^1H NMR of **1**

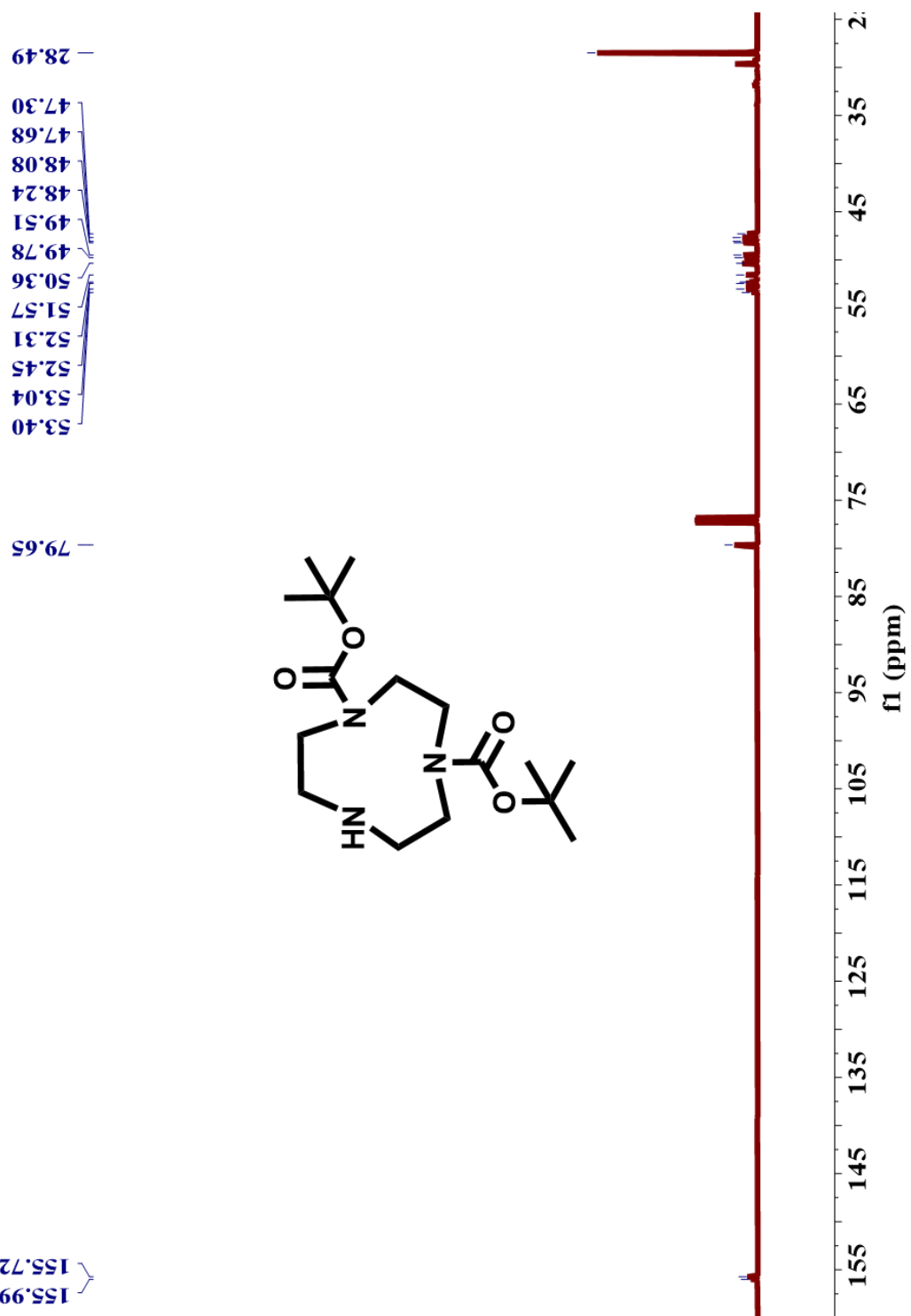


Figure S16. ^{13}C NMR of 1

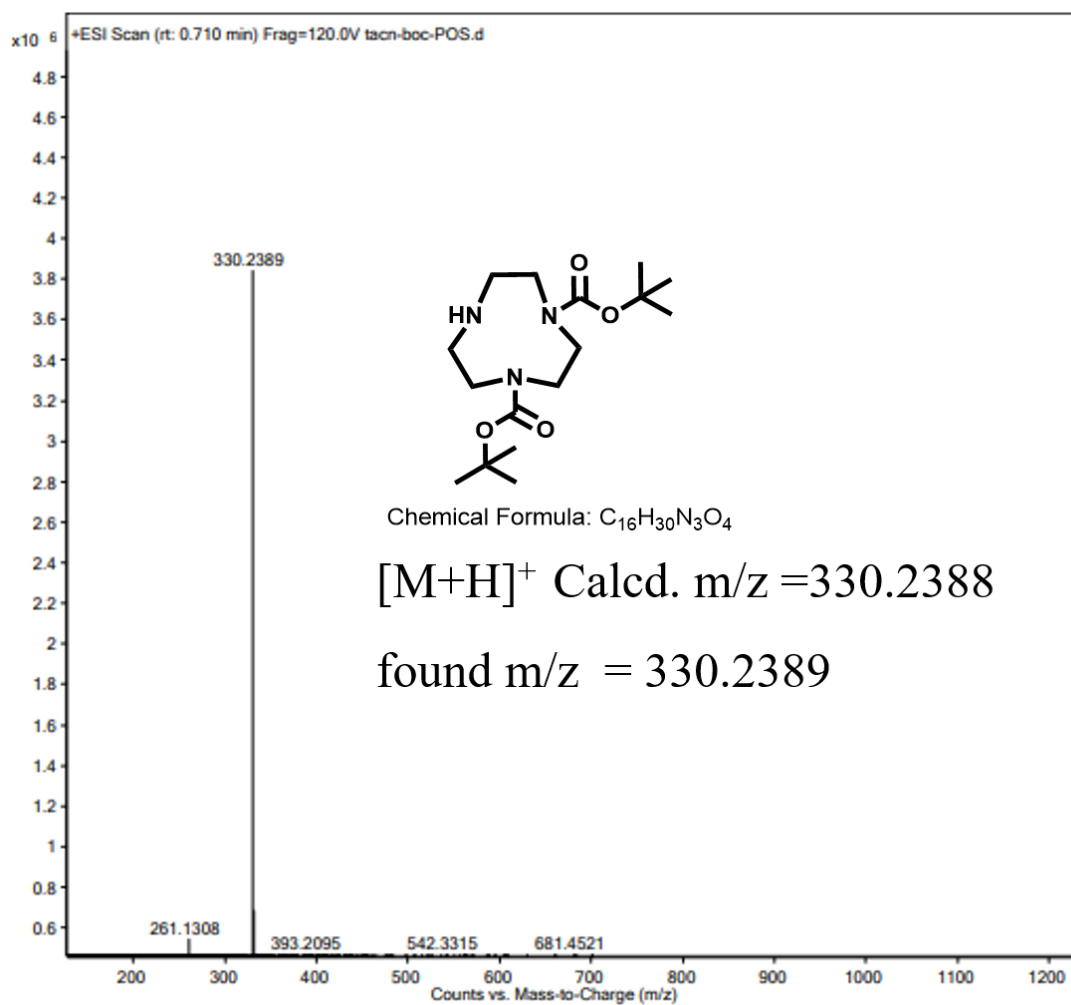


Figure S17. ESI-MS of 1

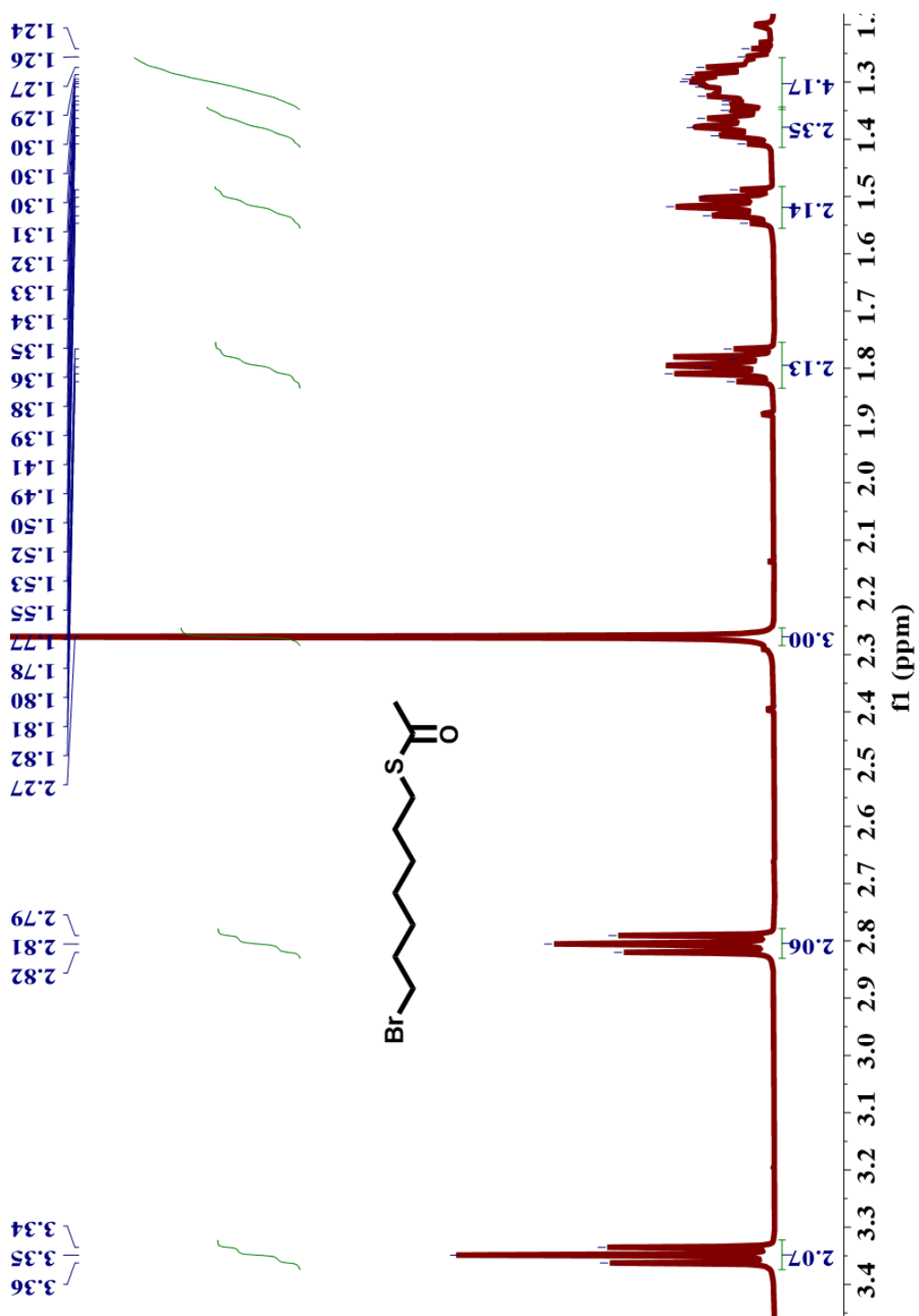


Figure S18. ^1H NMR of 2a

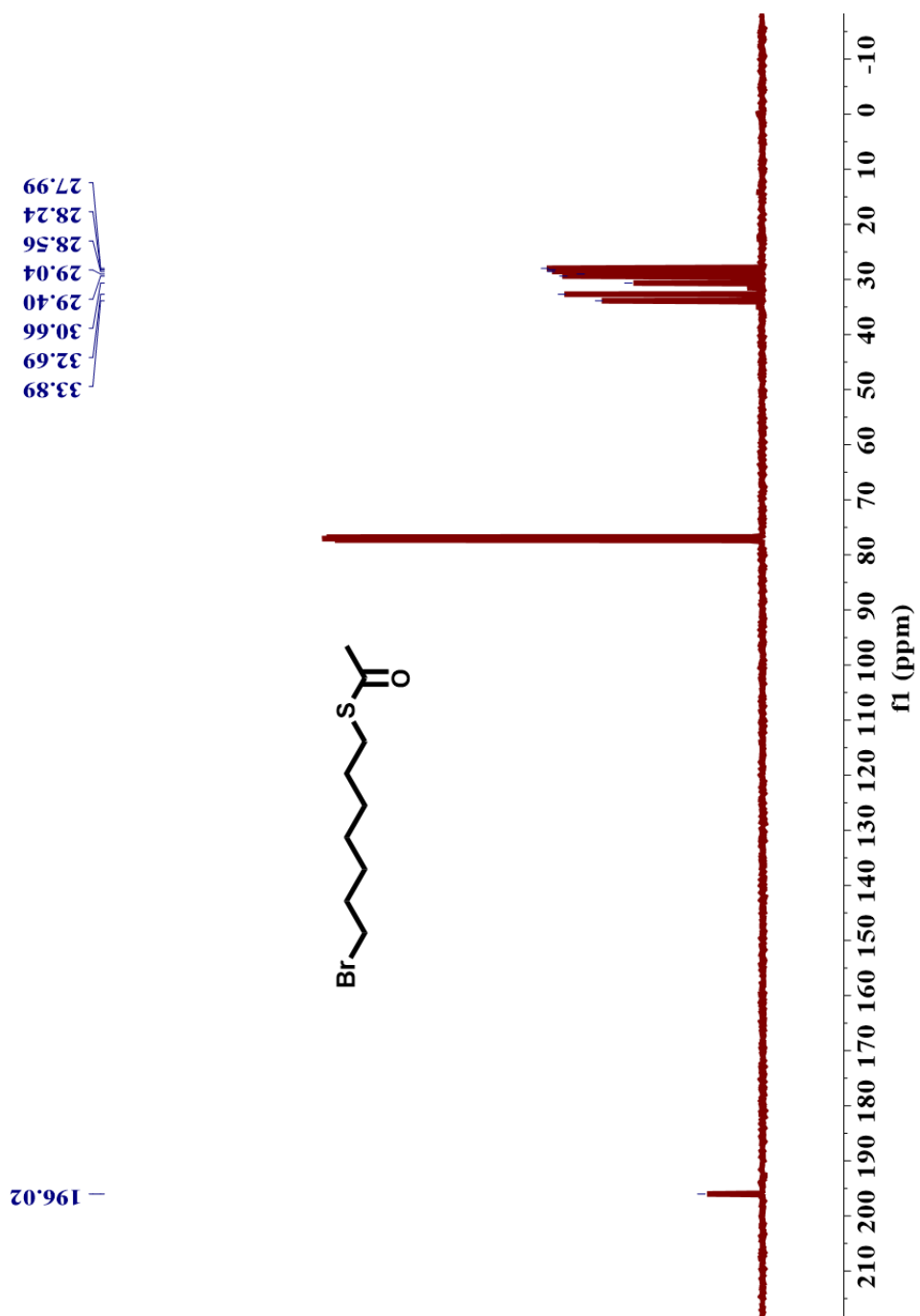


Figure S19. ^{13}C NMR of 2a

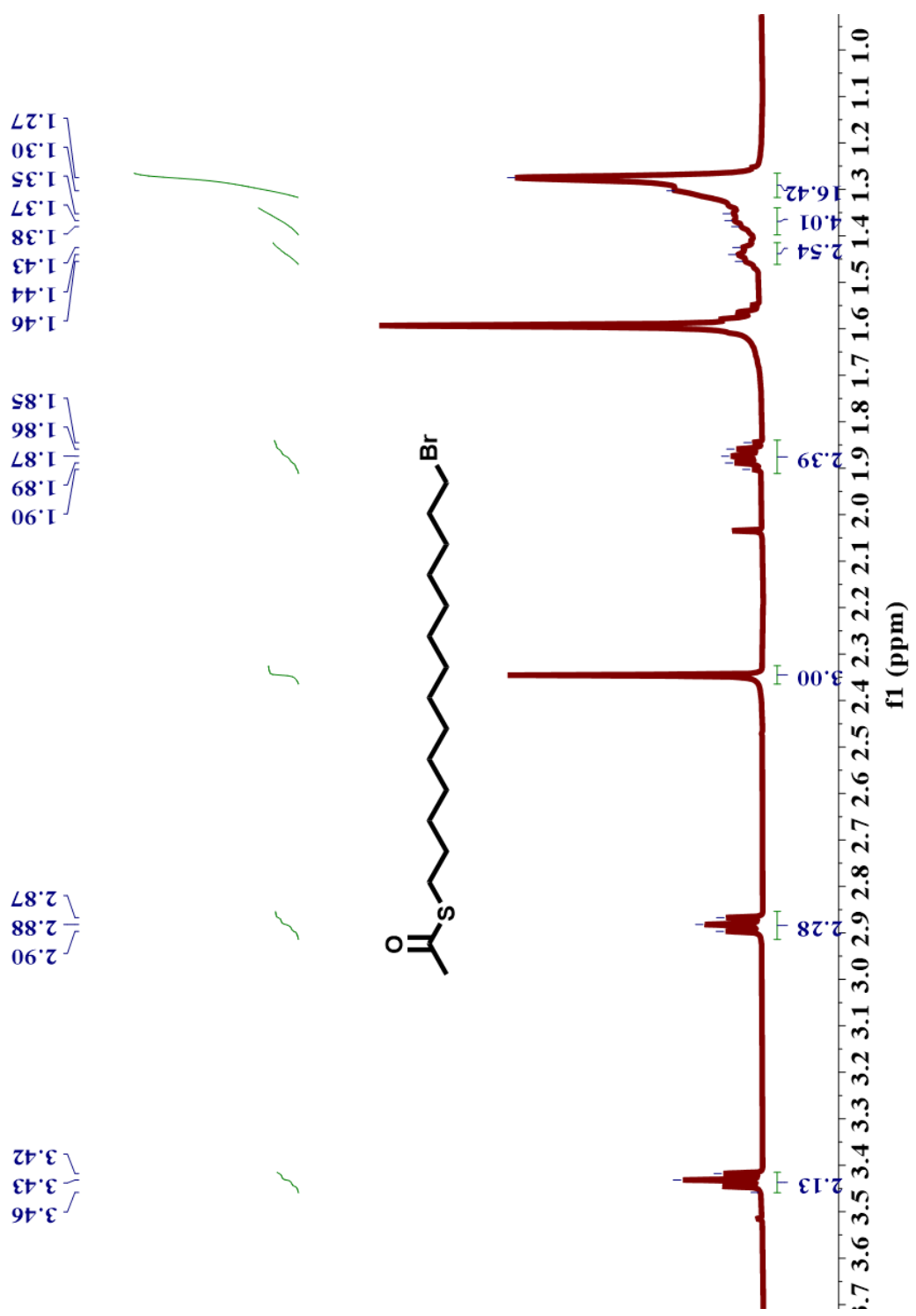


Figure S20. ¹H NMR of 2b

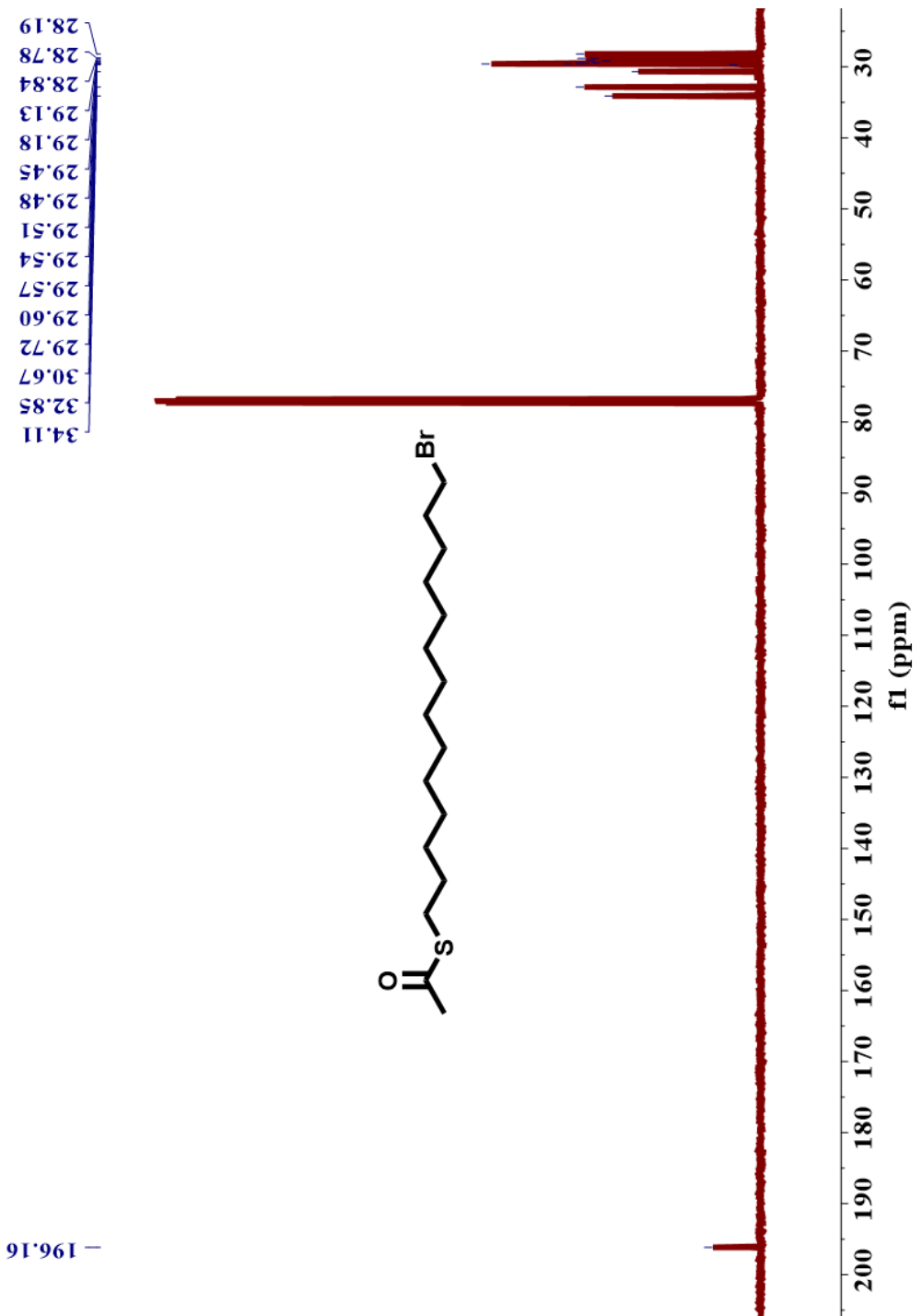


Figure S21. ¹³C NMR of 2b

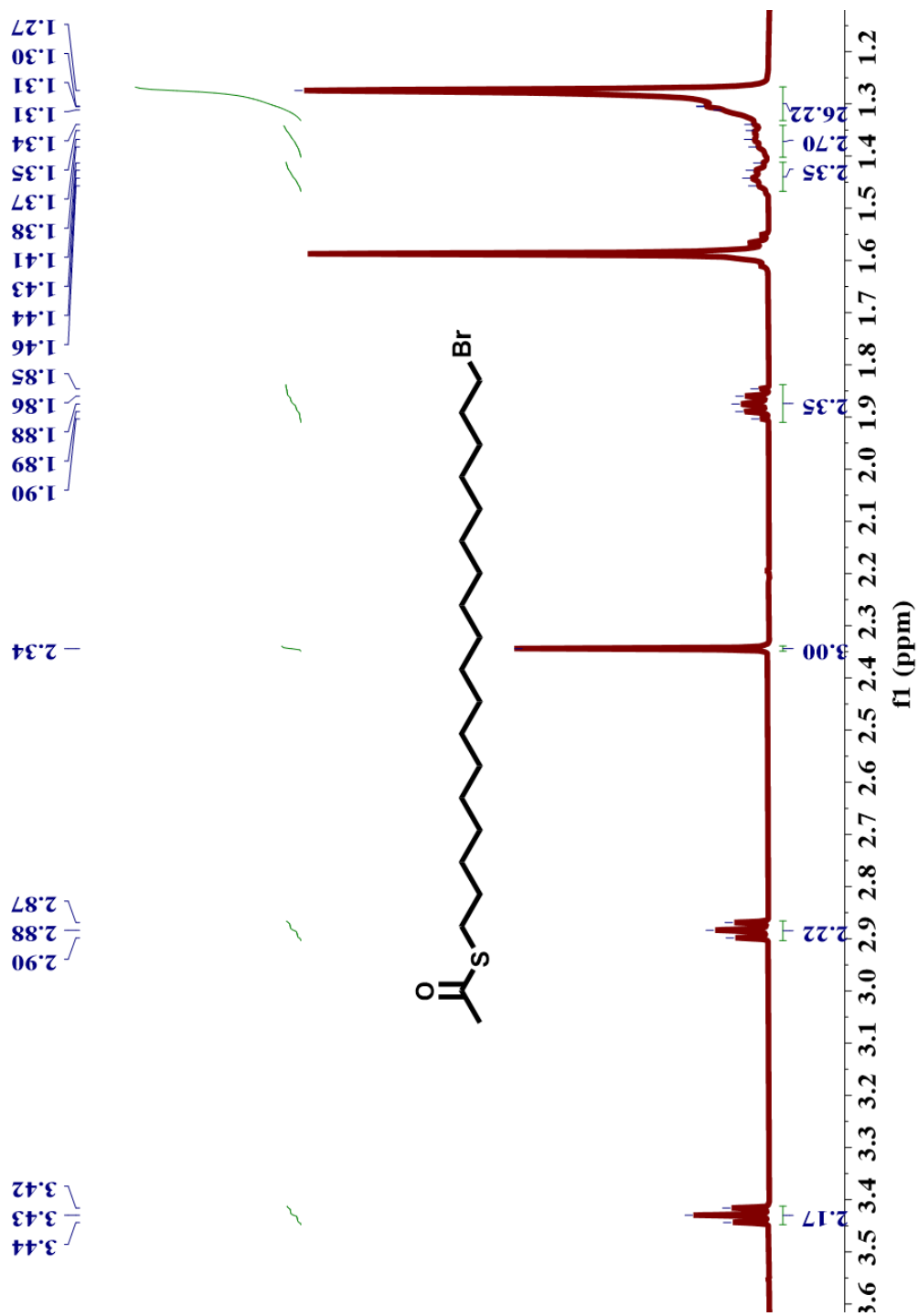


Figure S22. ^1H NMR of 2c

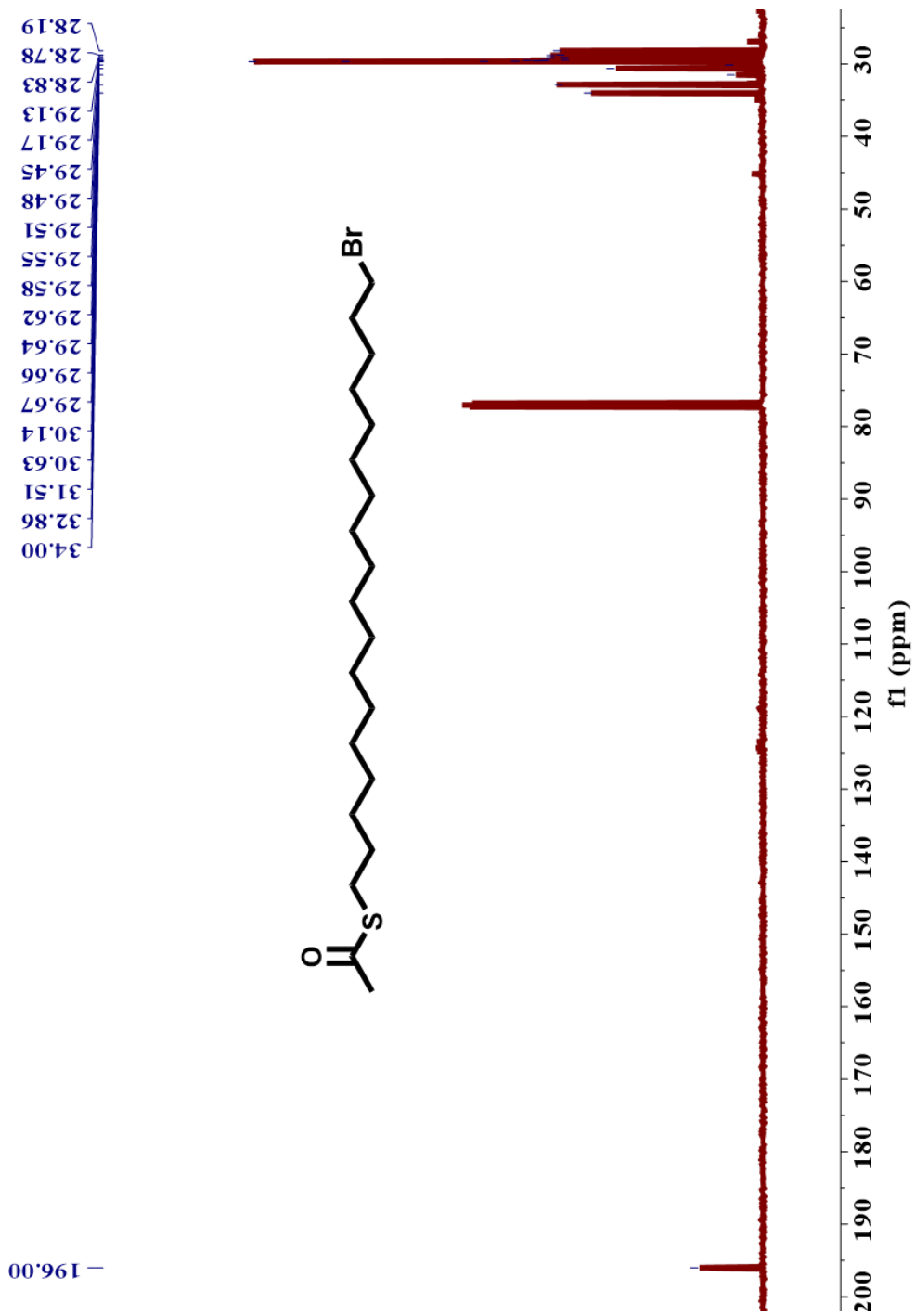


Figure S23. ^{13}C NMR of 2c

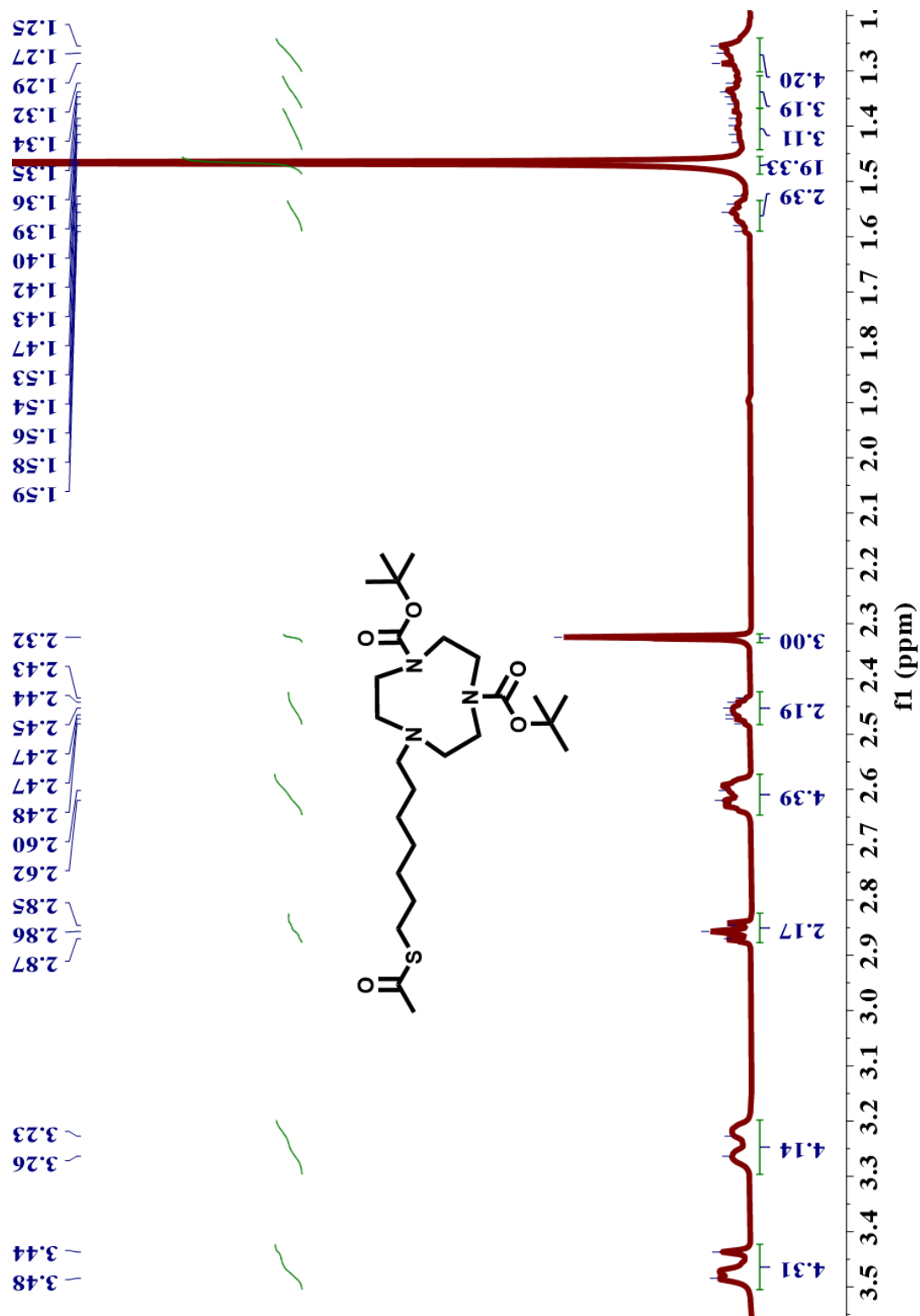


Figure S24. ¹H NMR of 3a

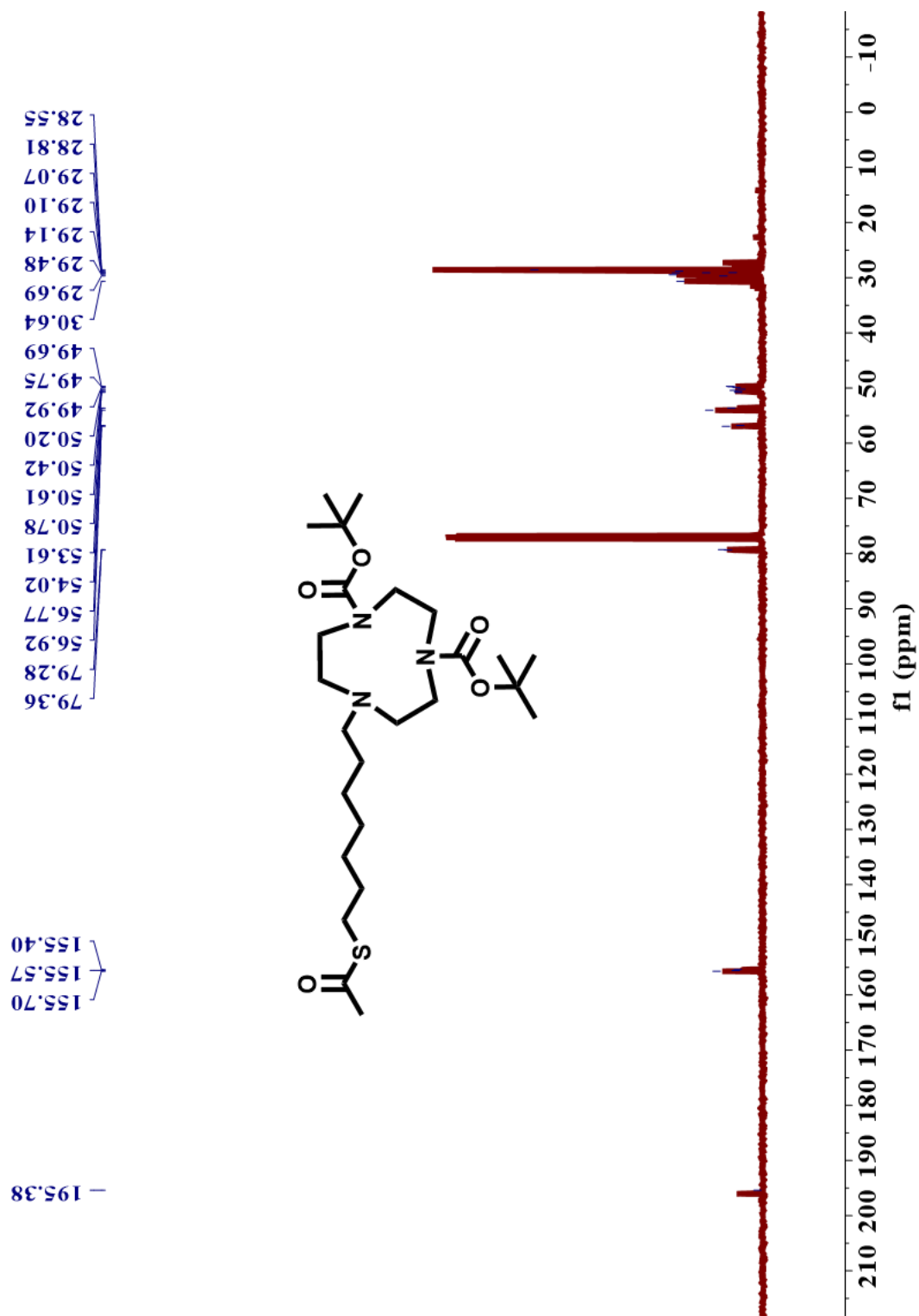


Figure S25. ^{13}C NMR of 3a

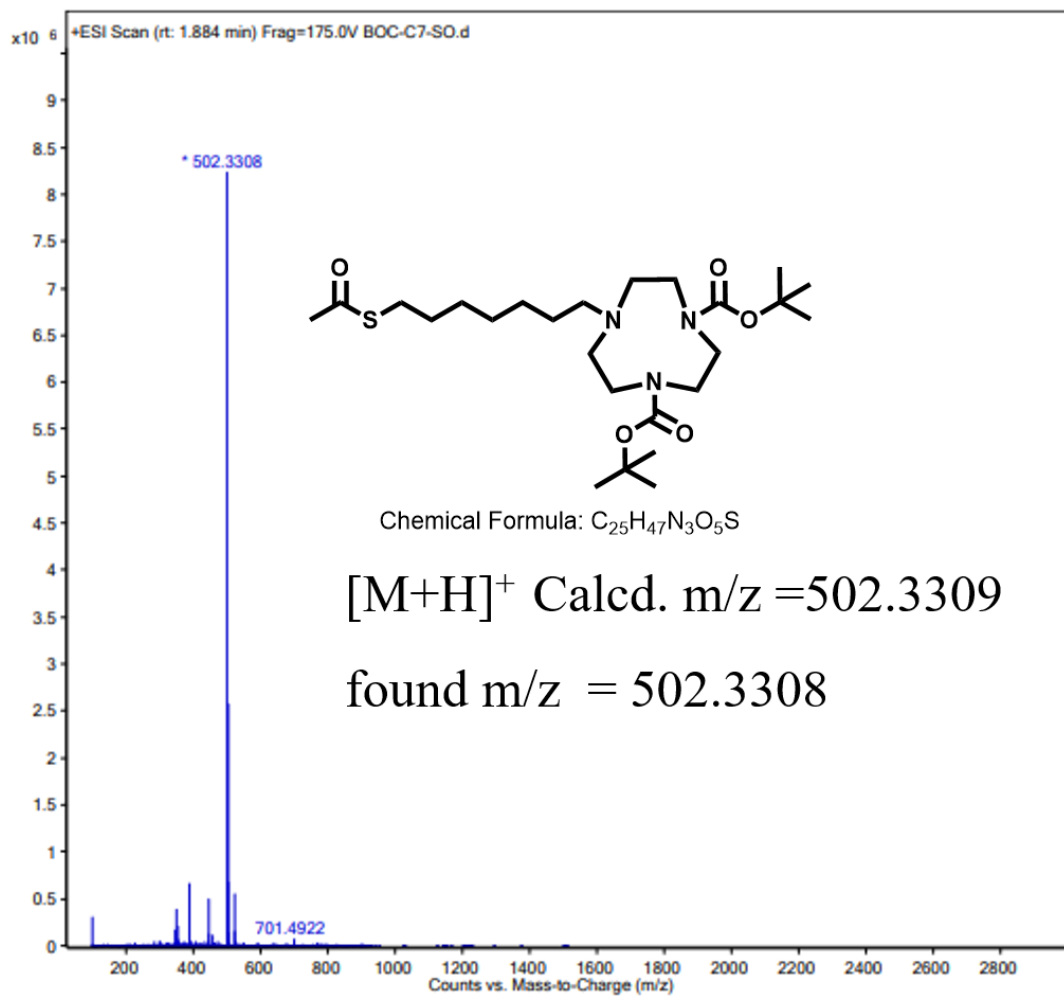


Figure S26. ESI-MS of 3a

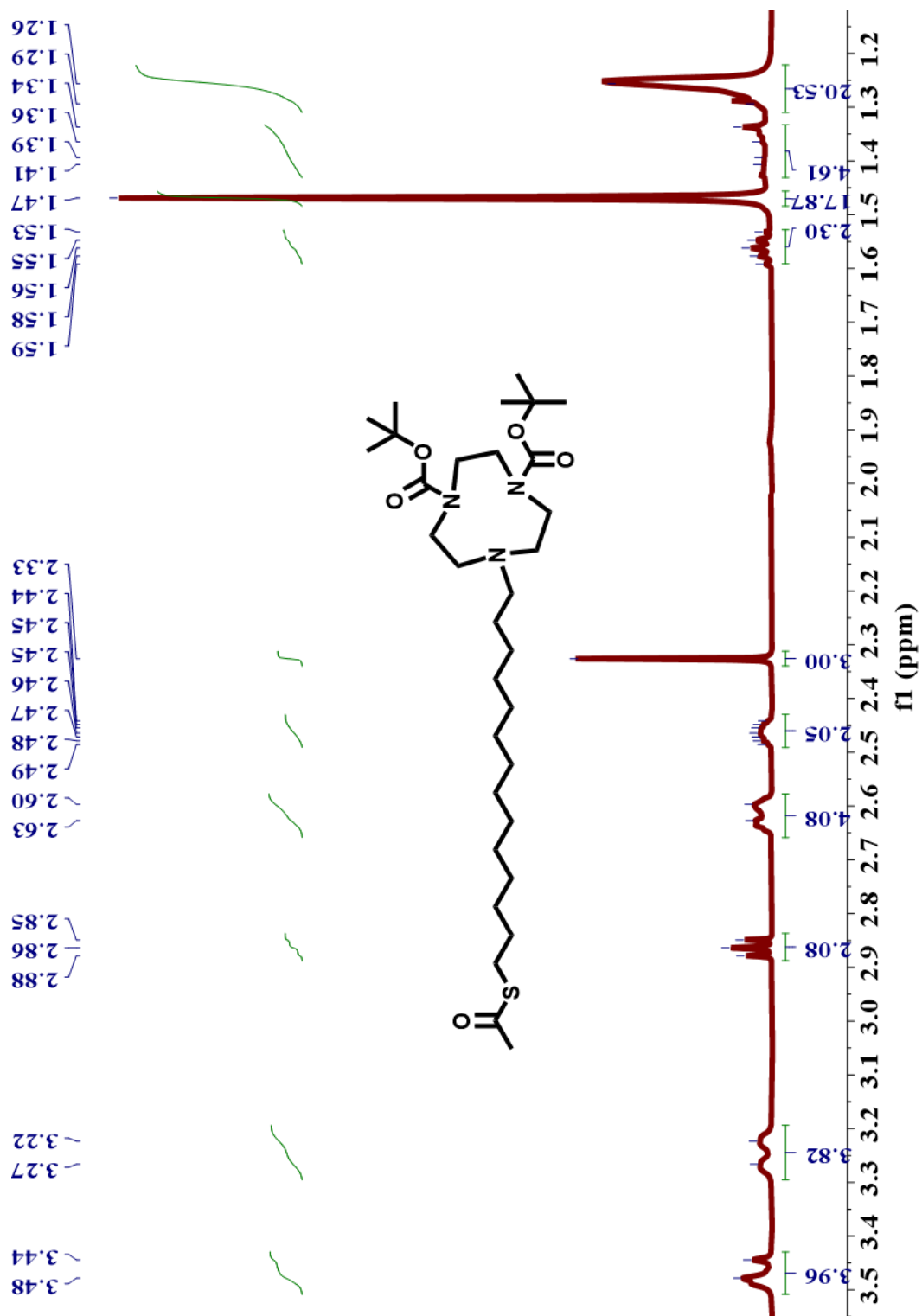


Figure S27. ^1H NMR of 3b

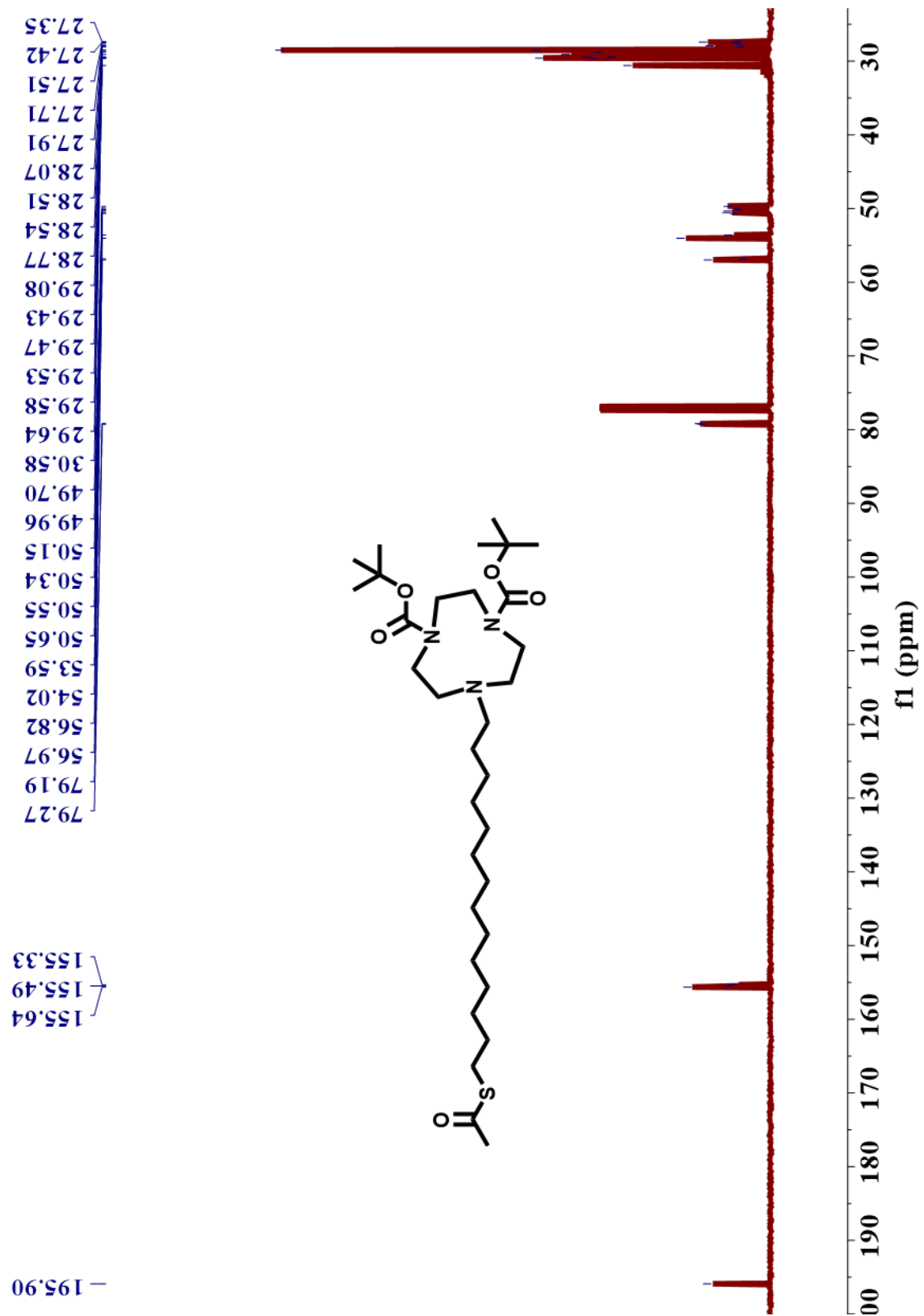


Figure S28. ^{13}C NMR of 3b

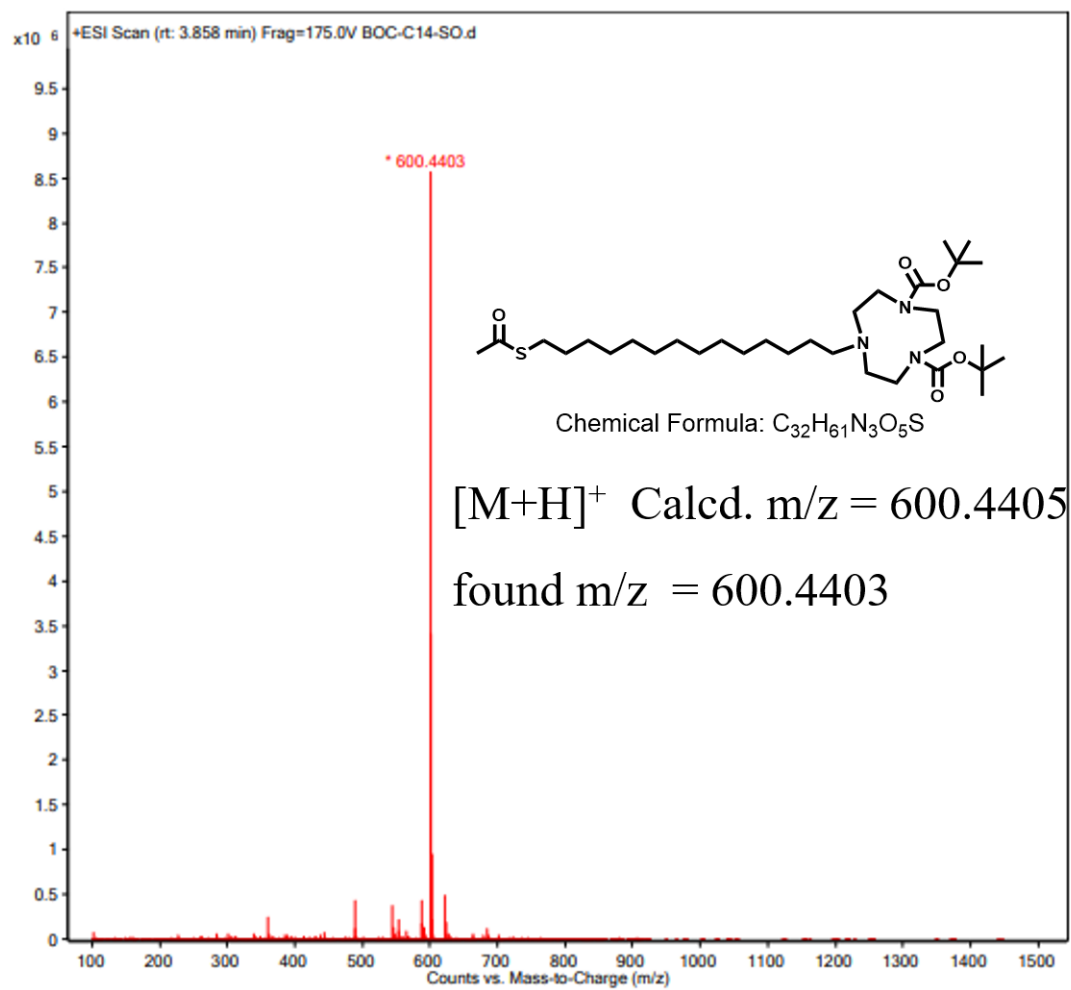


Figure S29. ESI-MS of 3b

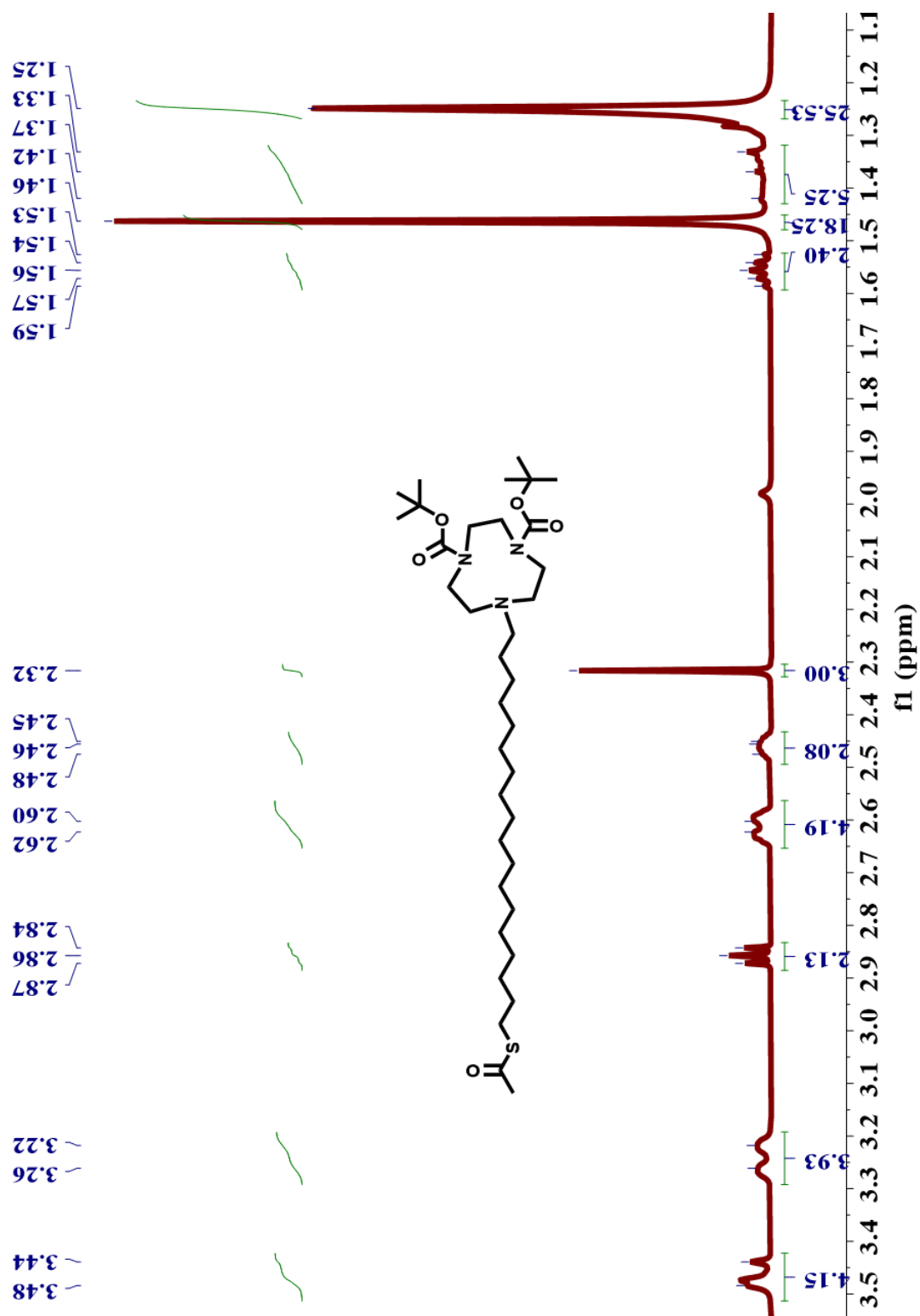


Figure S30. ^1H NMR of 3c

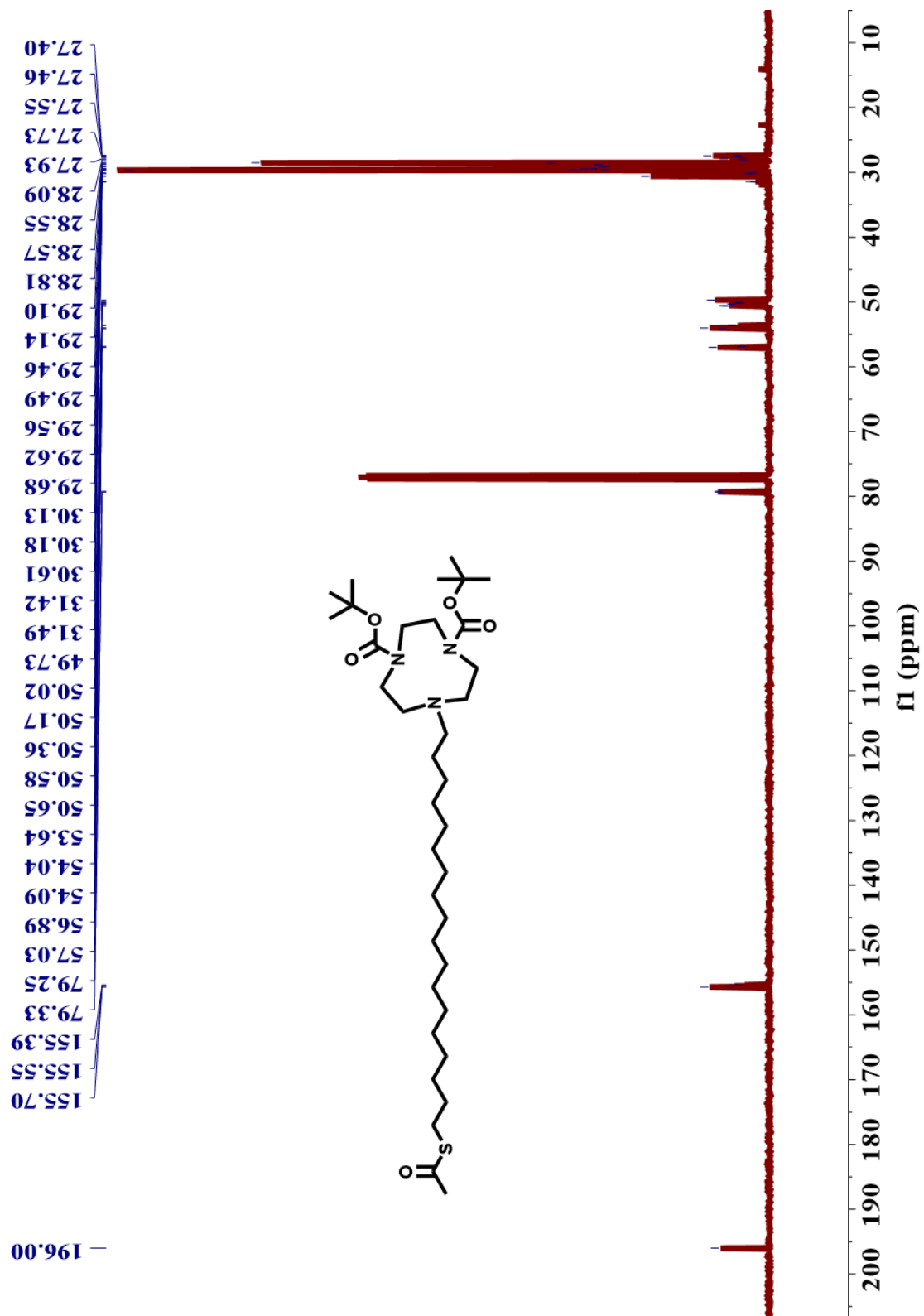


Figure S31. ^{13}C NMR of **3c**

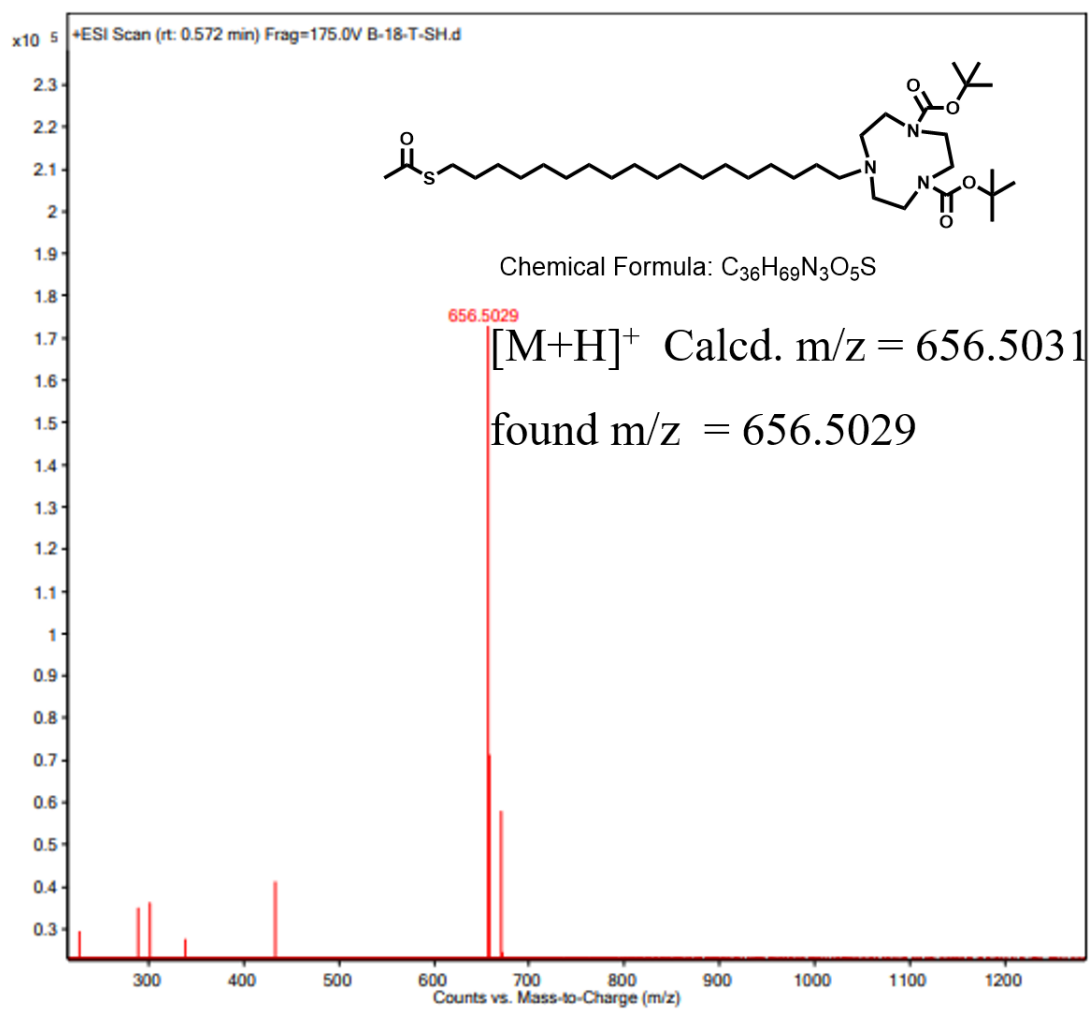


Figure S32. ESI-MS of 3c

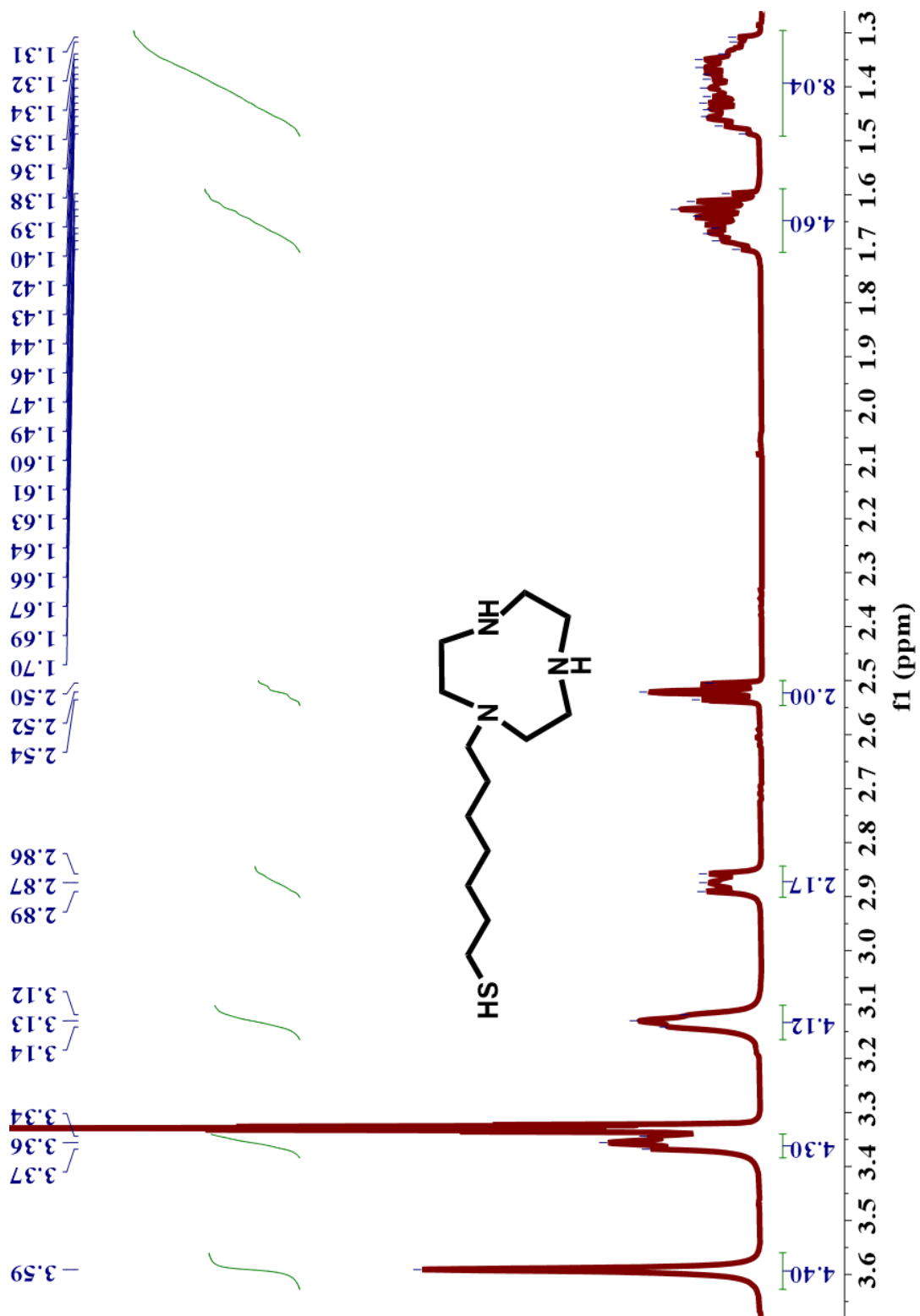


Figure S33. ^1H NMR of 4a

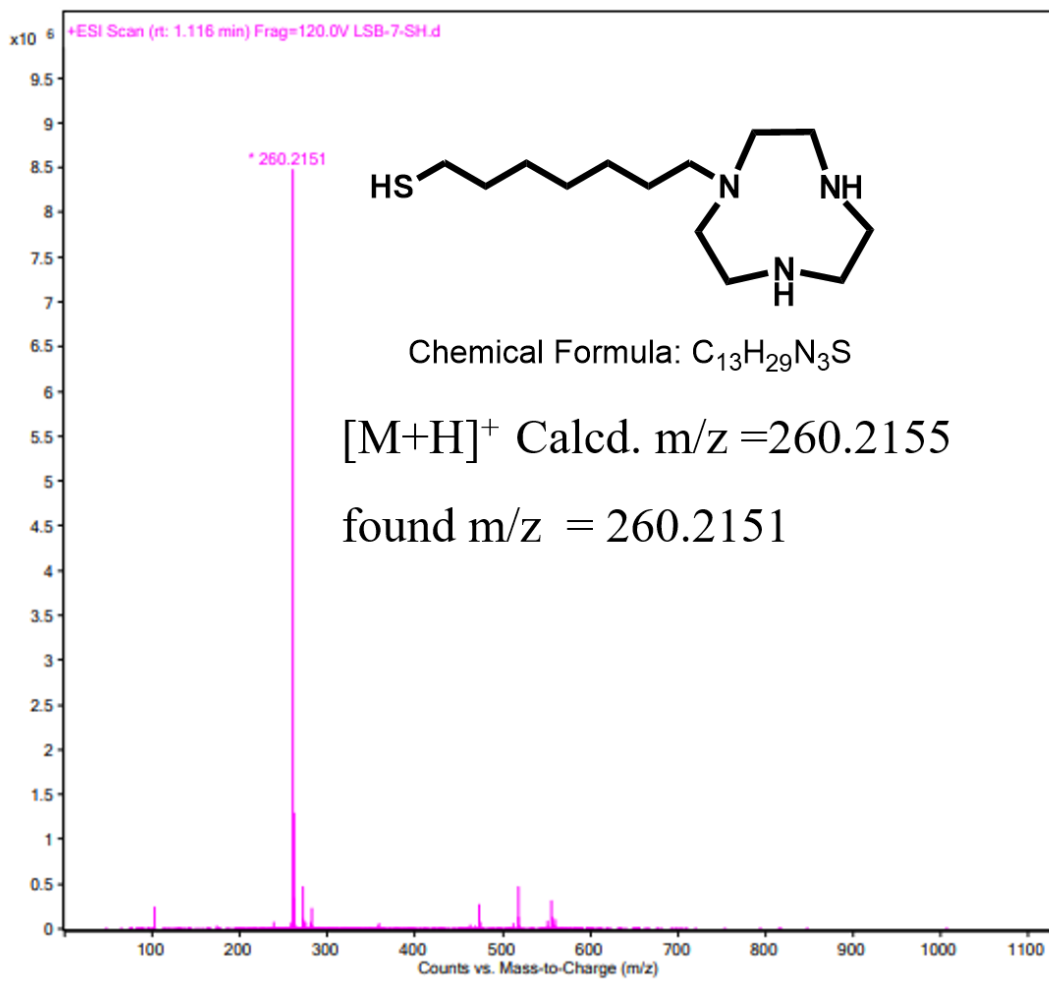


Figure S34. ESI-MS of 4a

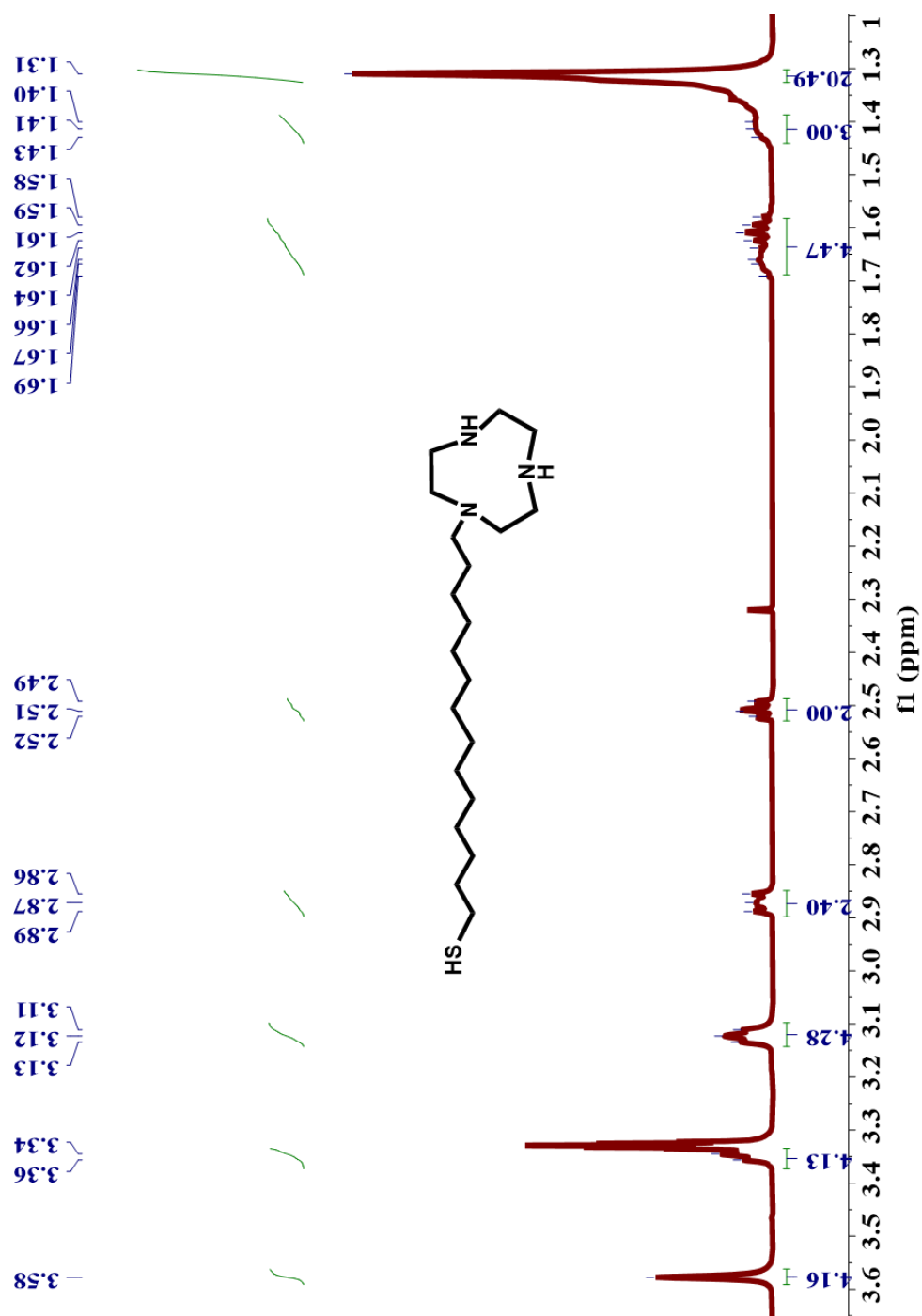


Figure S35. ^1H NMR of 4b

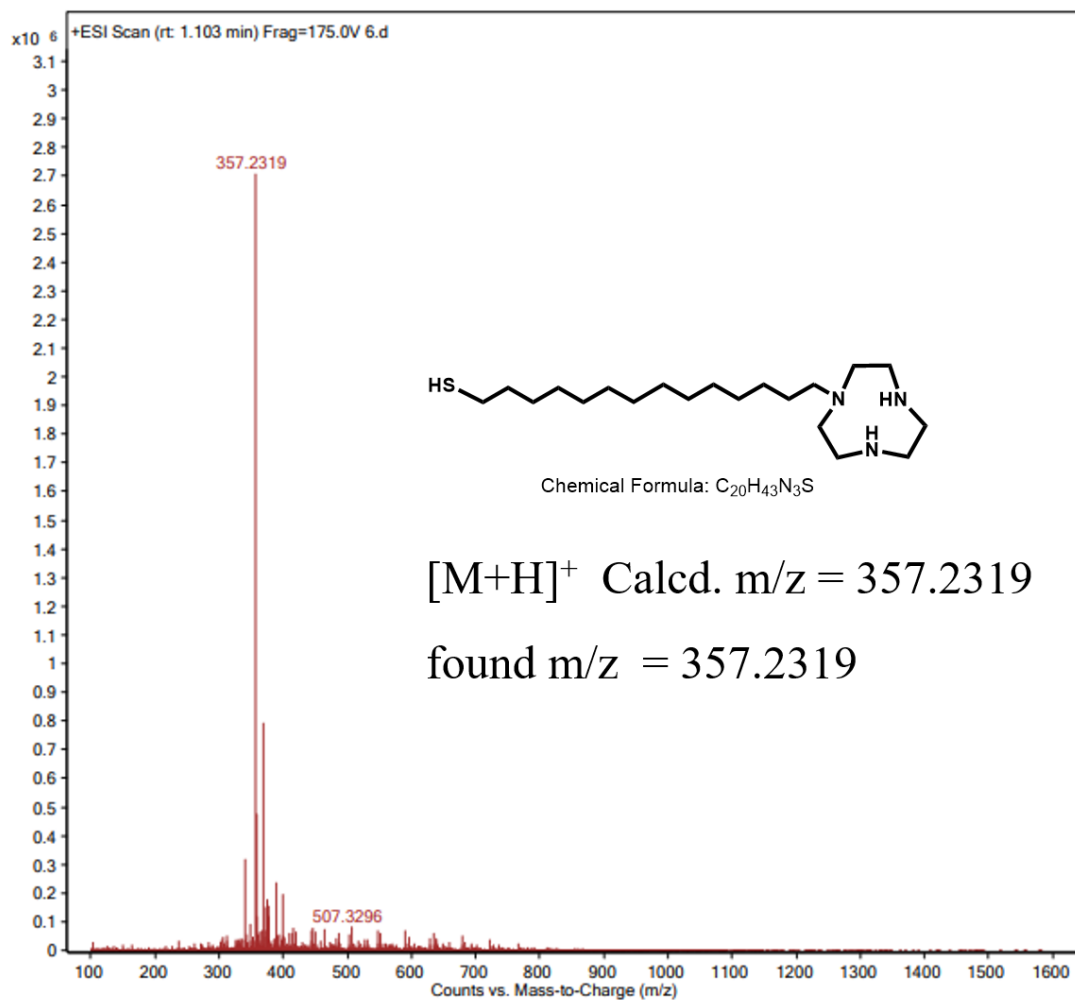


Figure S36. ESI-MS of 4b

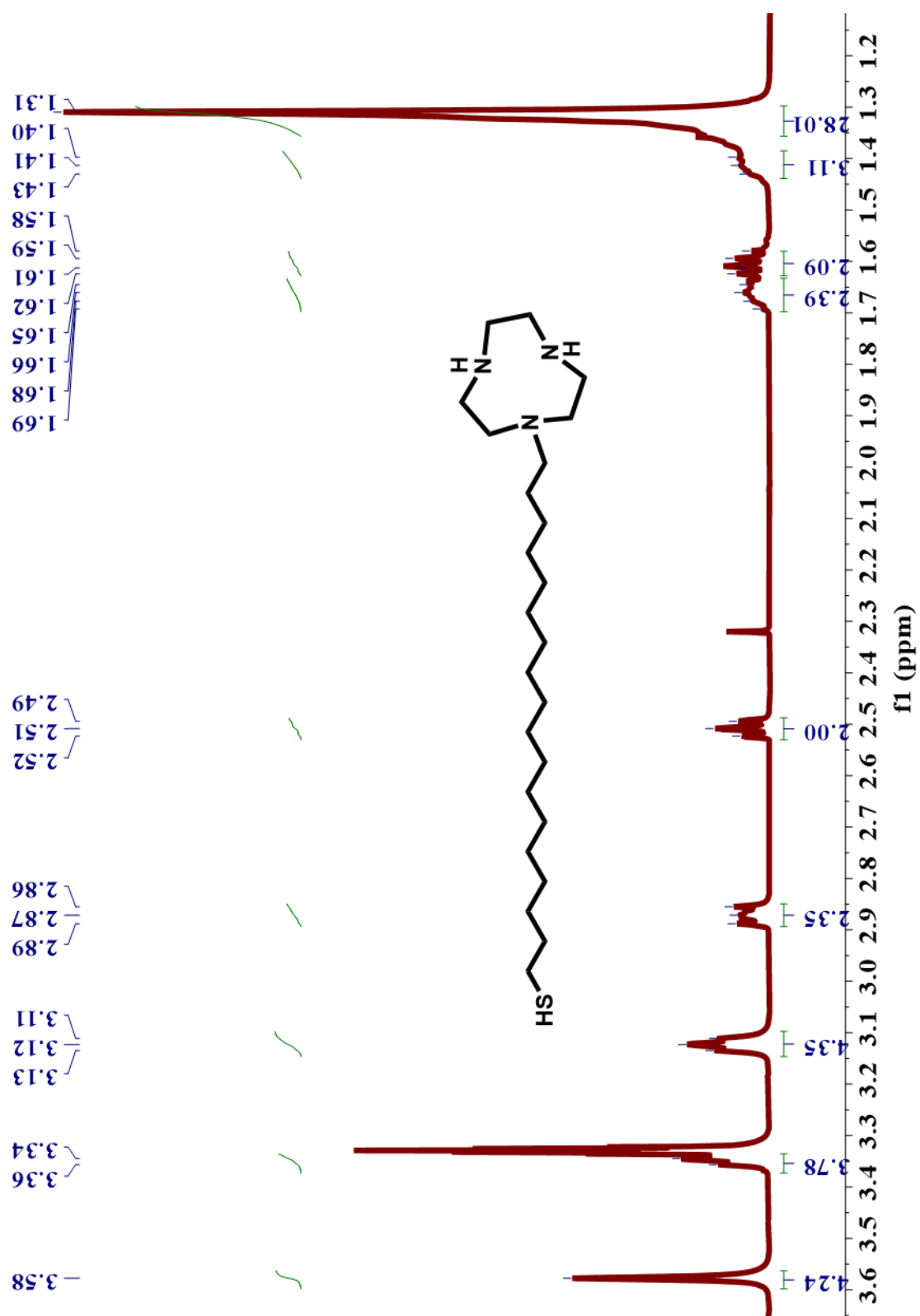


Figure S37. ^1H NMR of 4c

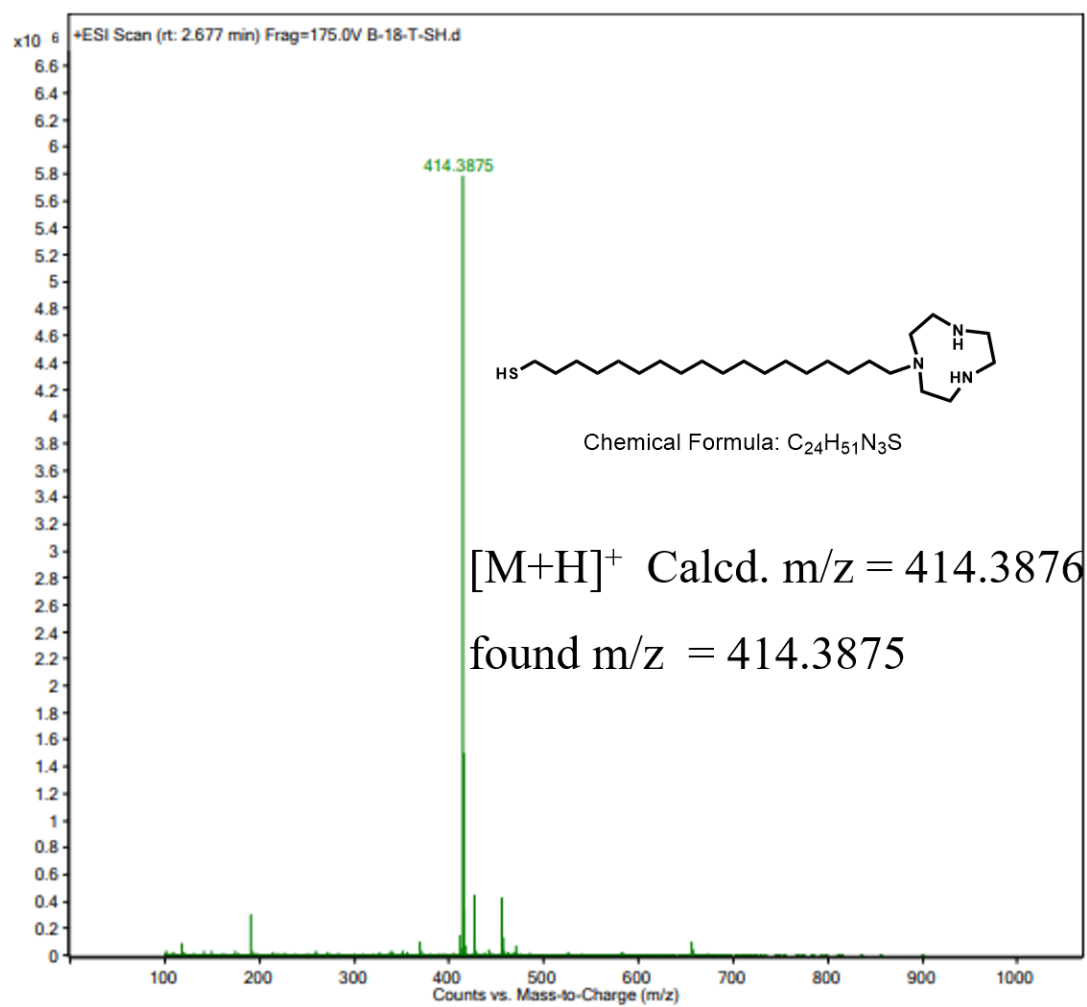


Figure S38. ESI-MS of **4c**

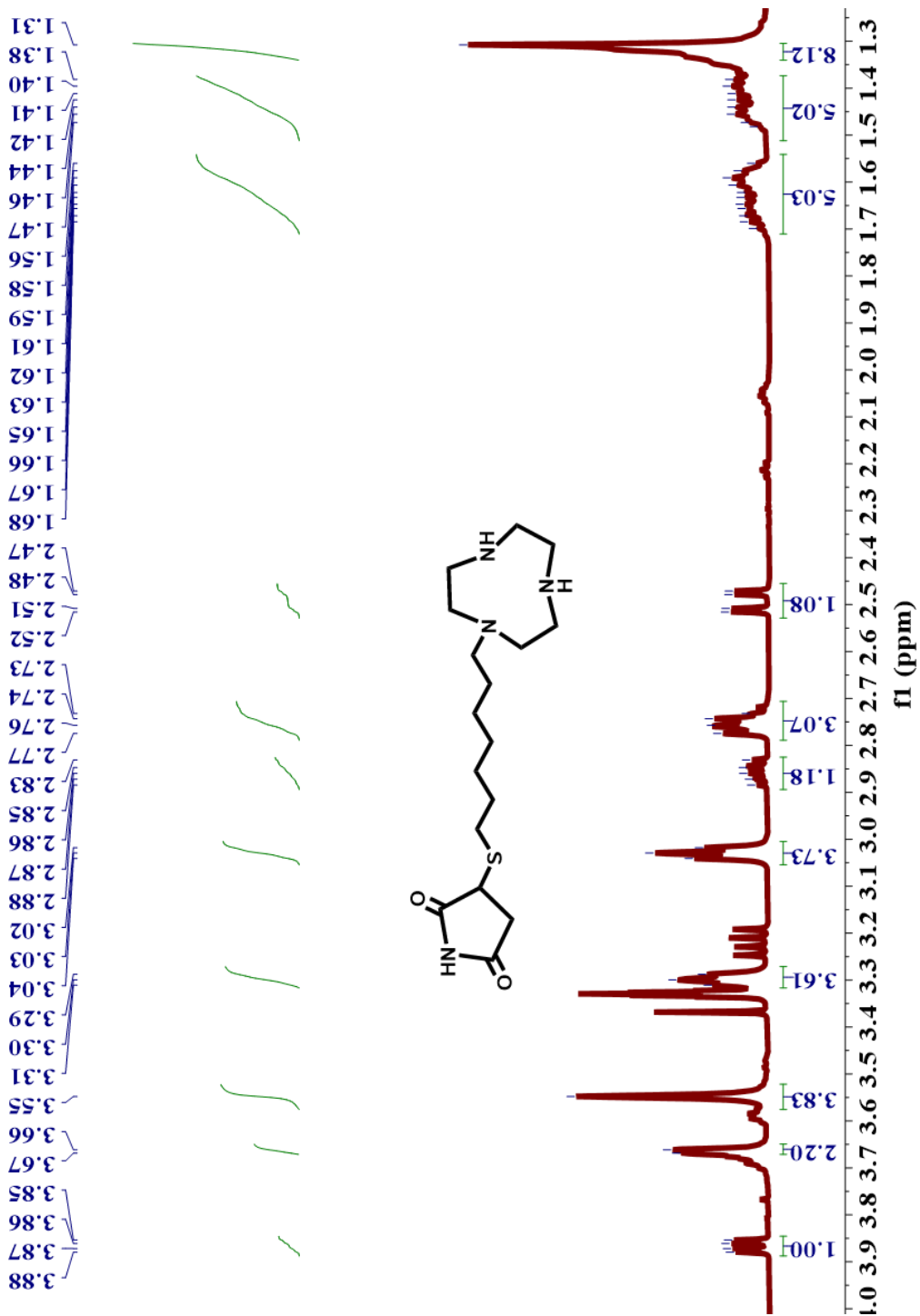


Figure S39. ¹H NMR of TACN-C₇-S-Succinimide

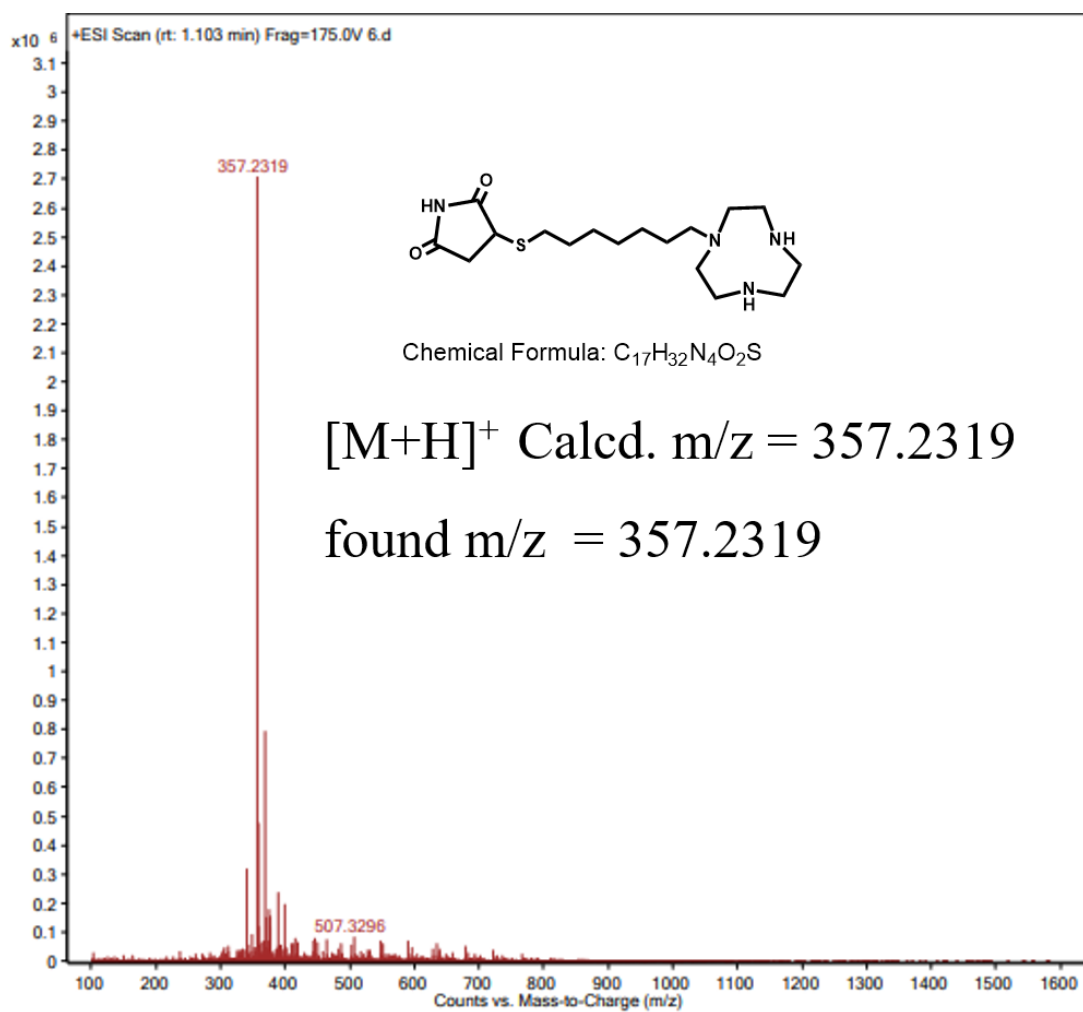


Figure S40. ESI-MS of TACN-C₇-S-Succinimide

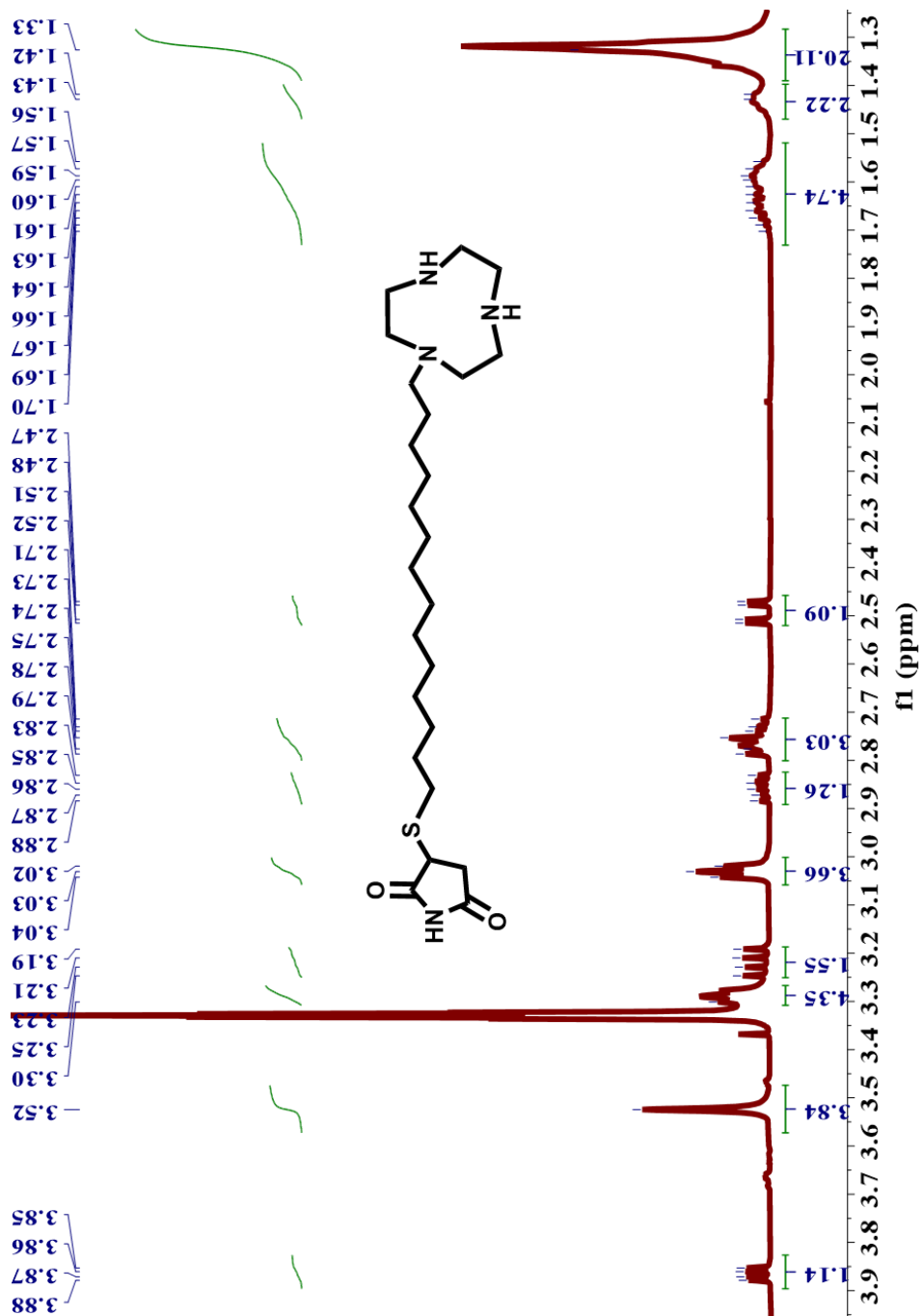


Figure S41. ¹H NMR of TACN-C₁₄-S-Succinimide

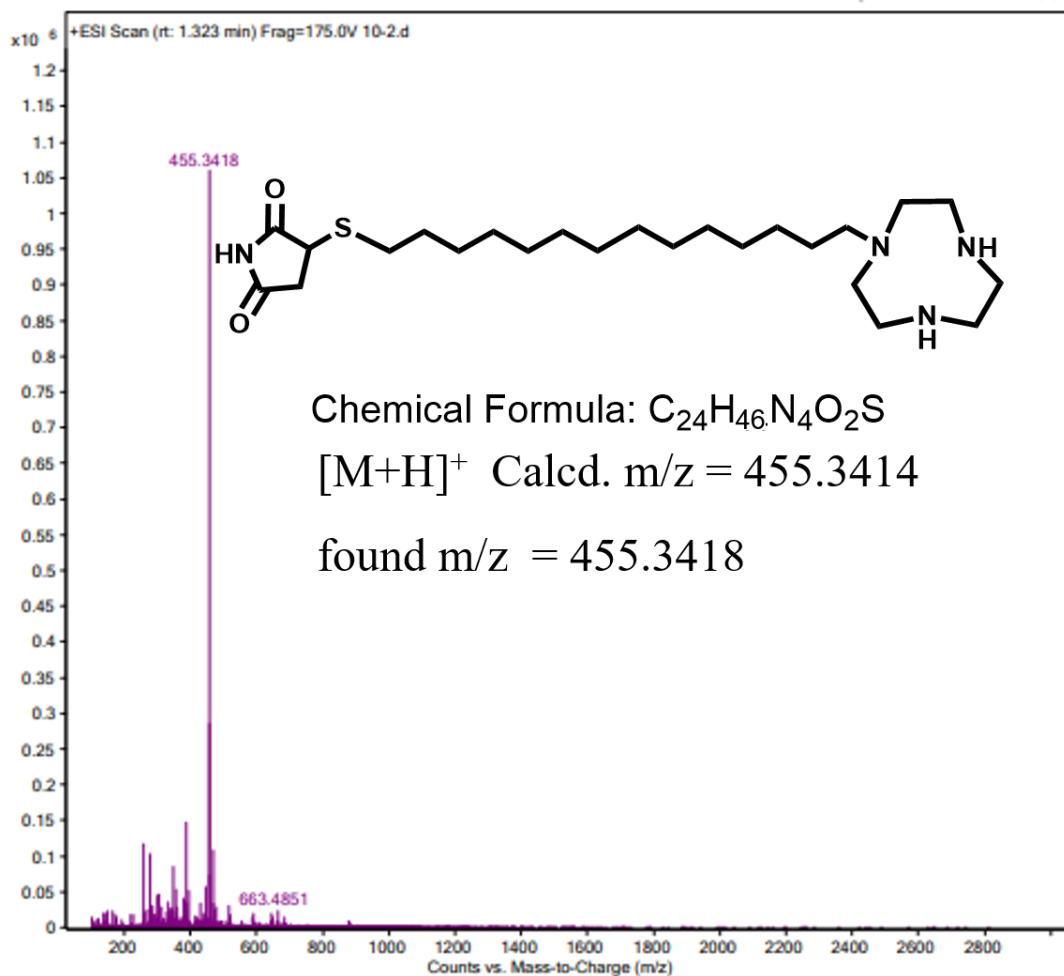


Figure S42. ESI-MS of TACN-C₁₄-S-Succinimide

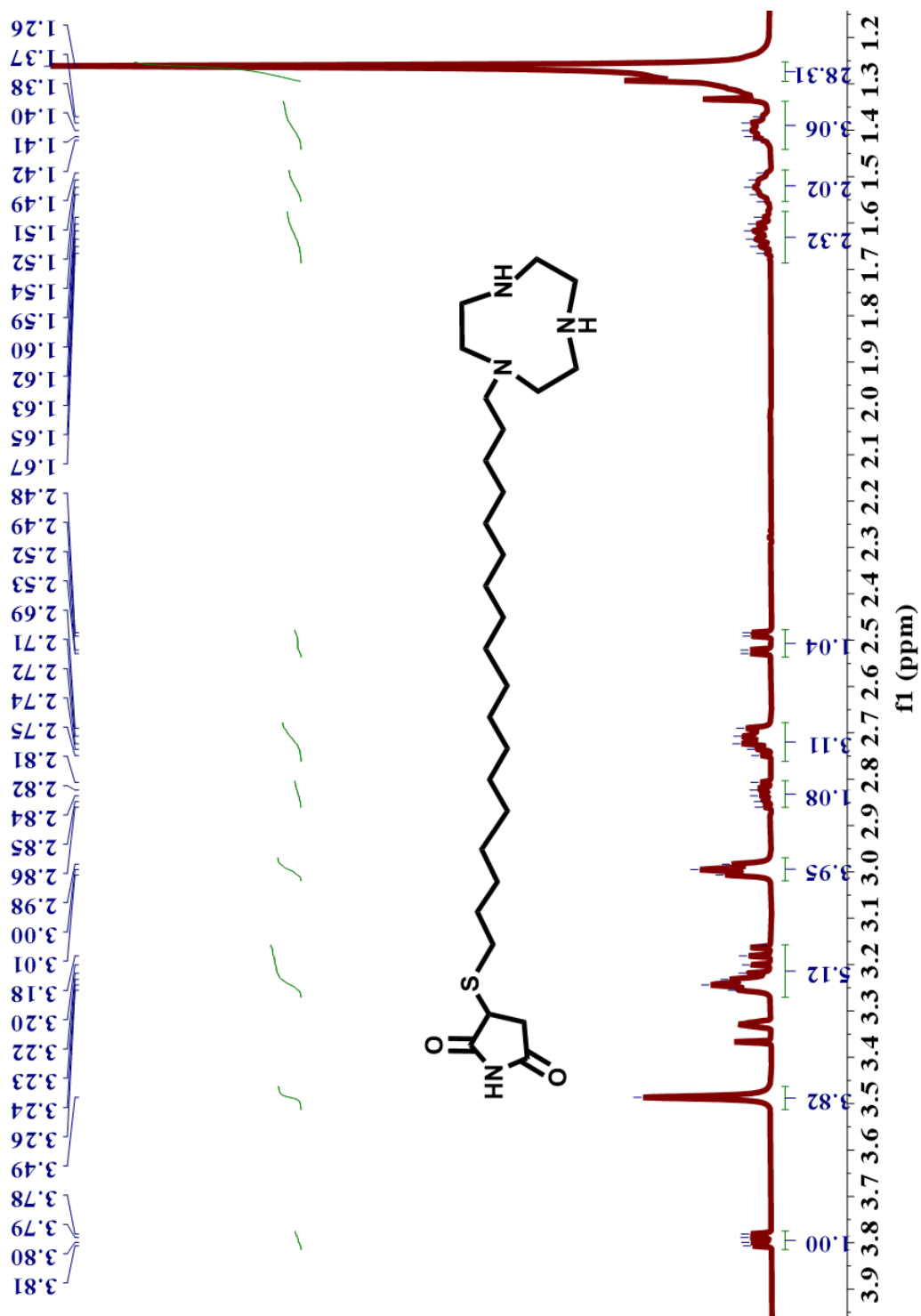


Figure S43. ^1H NMR of TACN-C₁₈-S-Succinimide

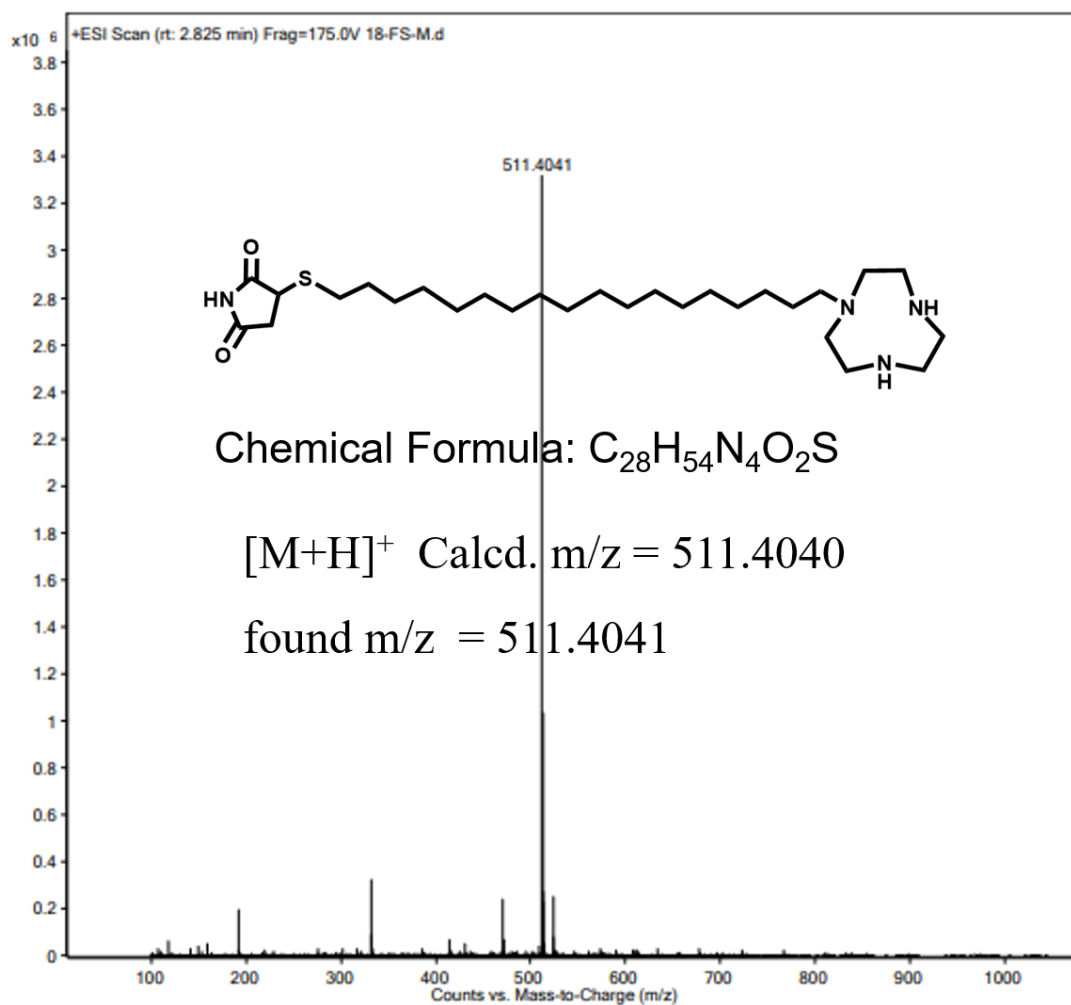


Figure S44. ESI-MS of TACN-C₁₈-S-Succinimide

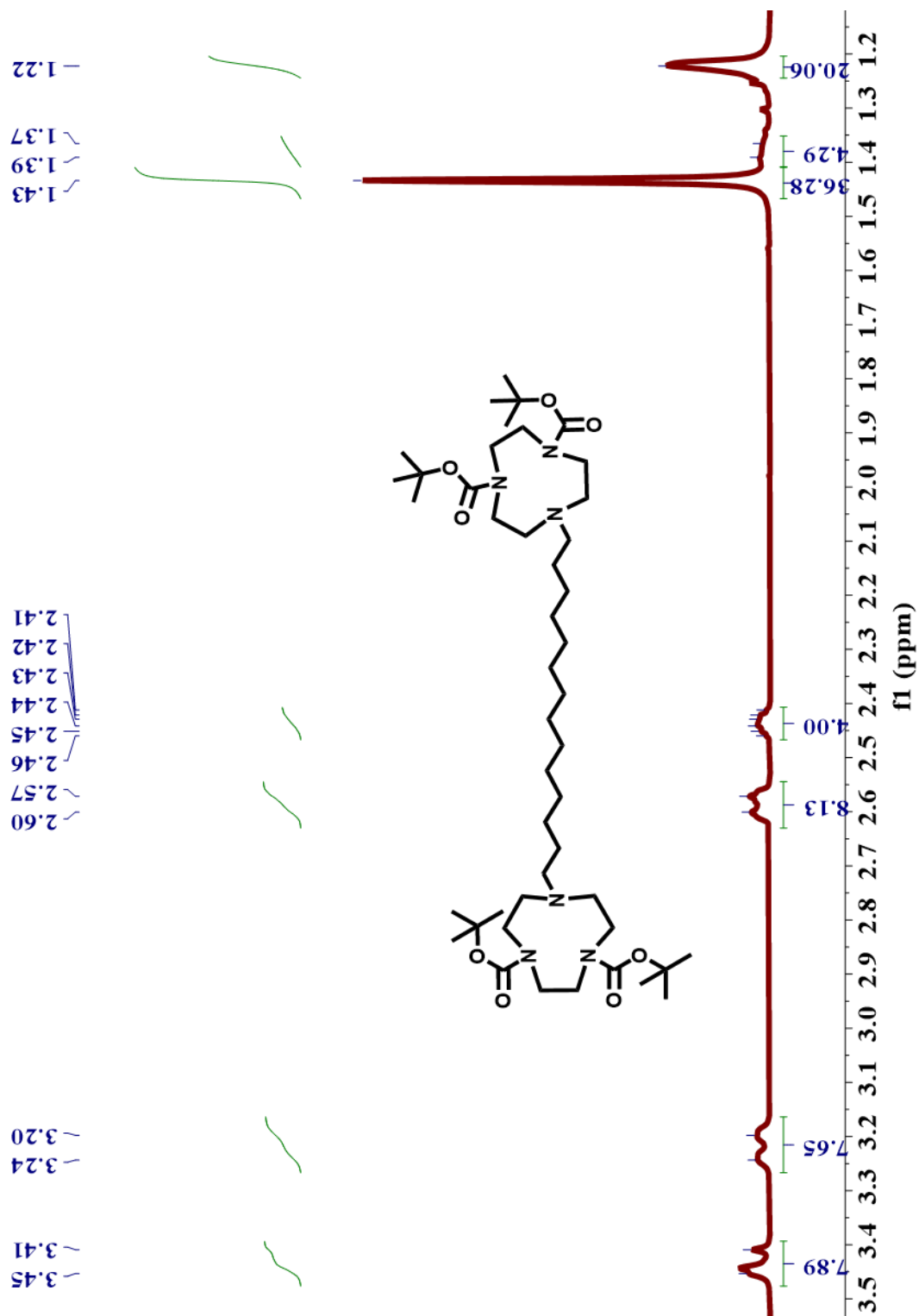


Figure S45. ^1H NMR of **6**

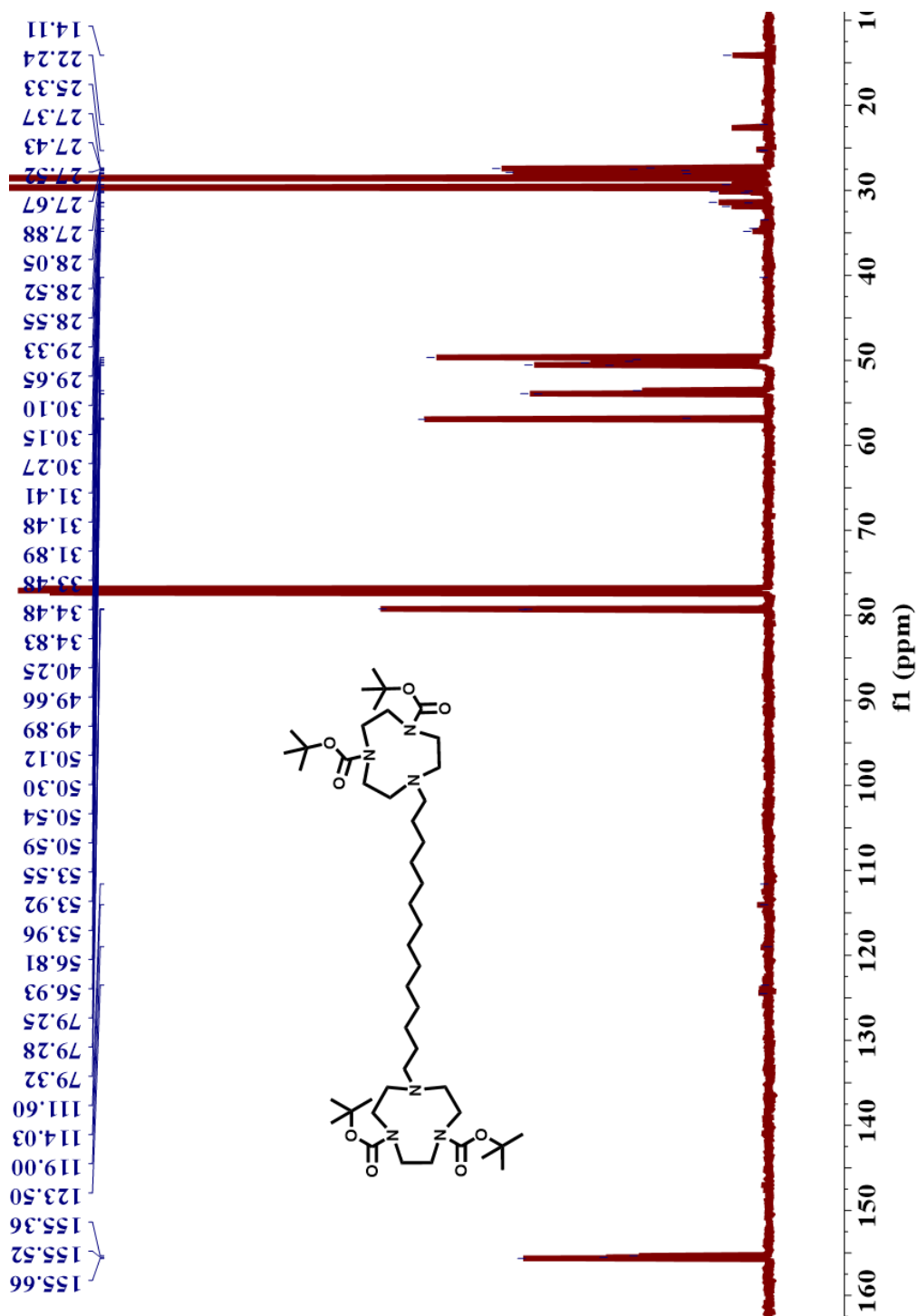


Figure S46. ¹³C NMR of 6

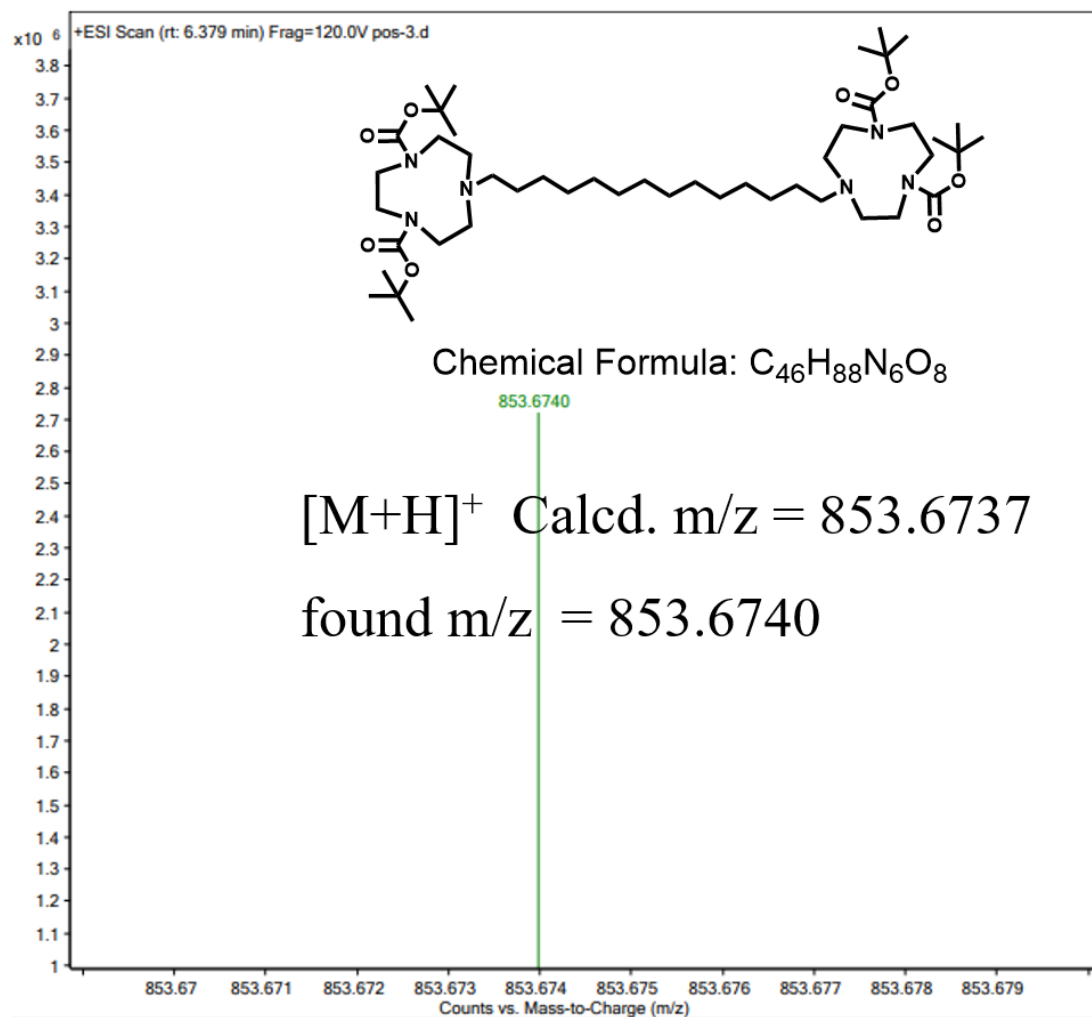


Figure S47. ESI-MS of 6

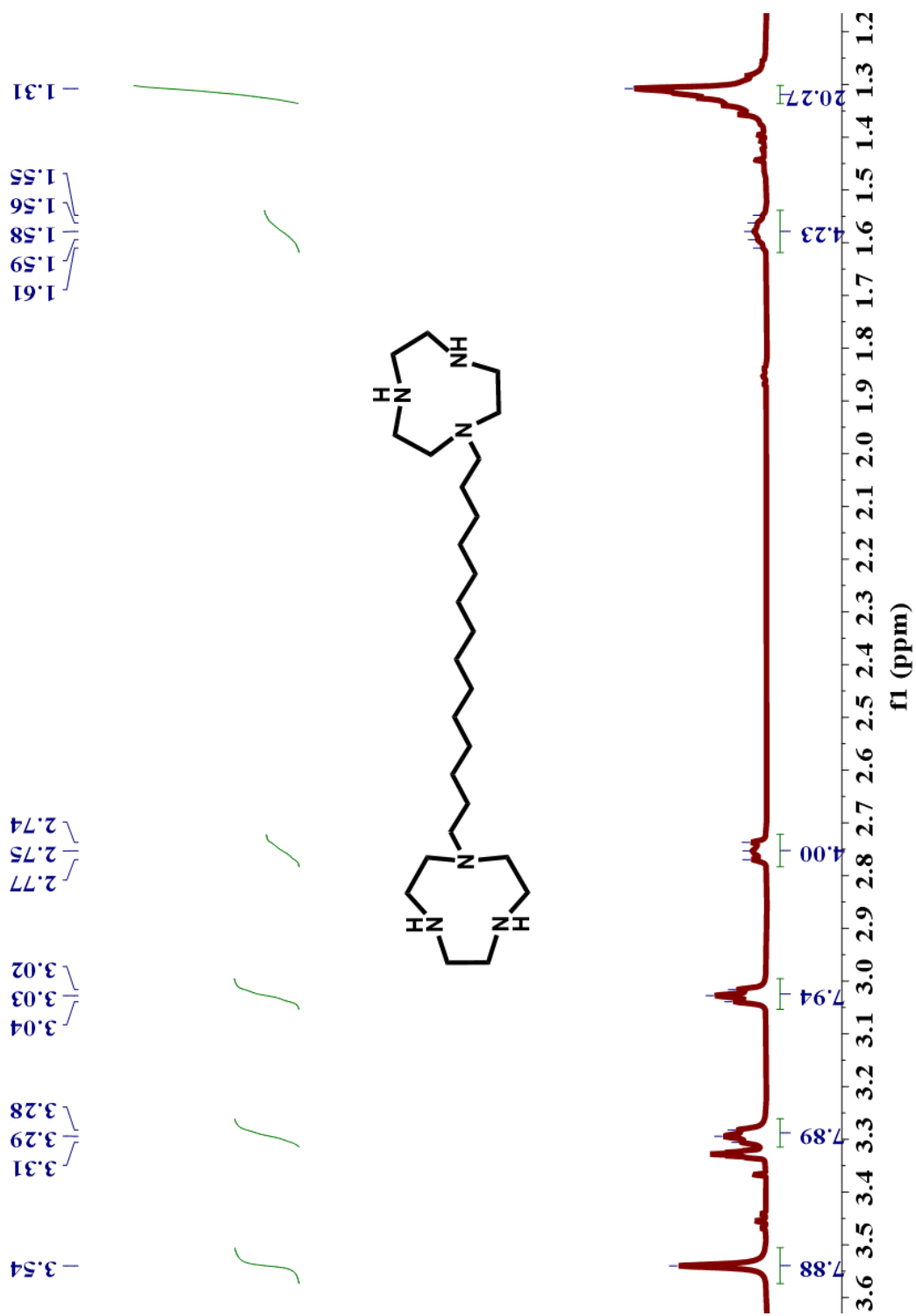


Figure S48. ^1H NMR of TACN-C₁₄-TACN

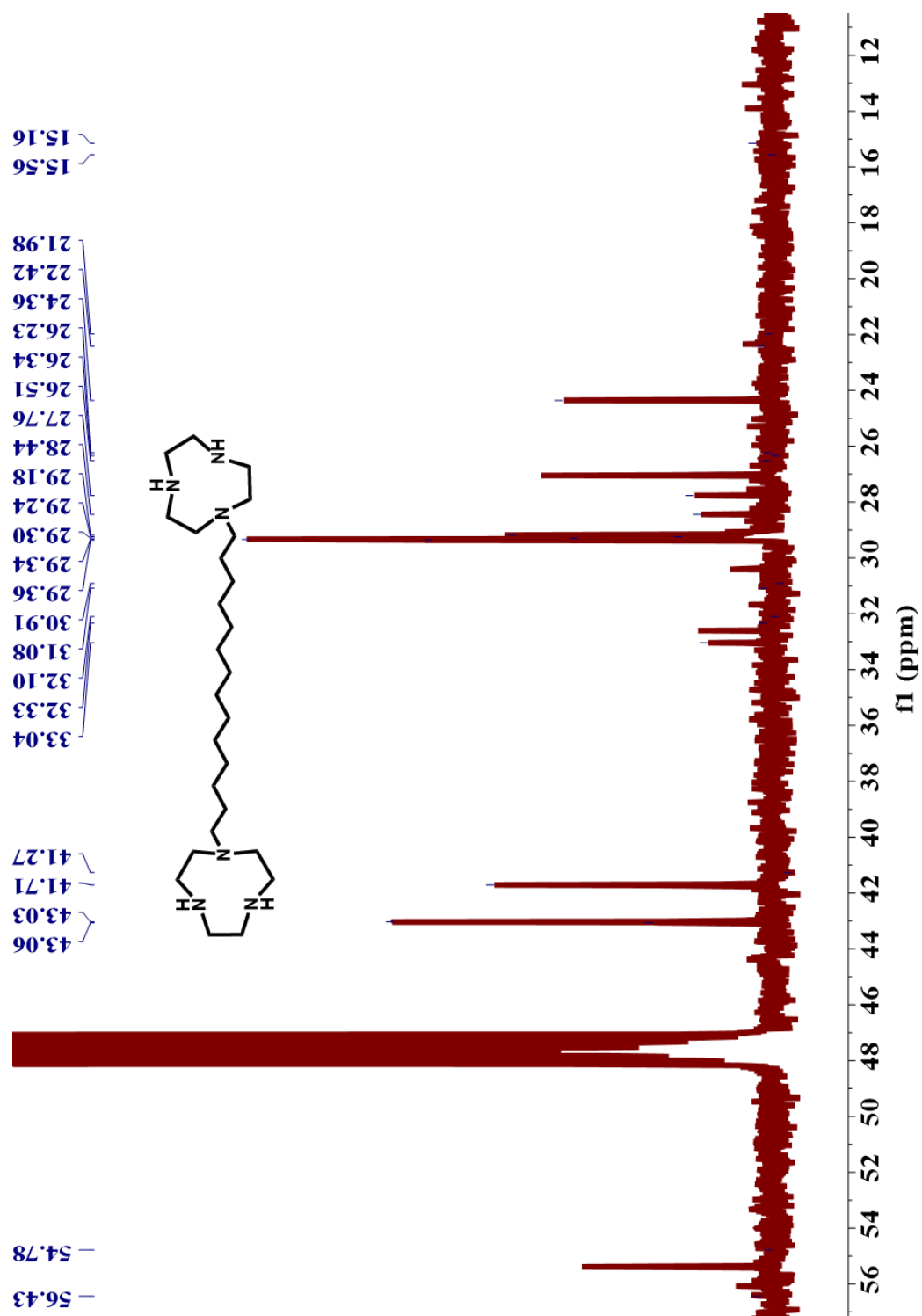


Figure S49. ^{13}C NMR of TACN-C₁₄-TACN

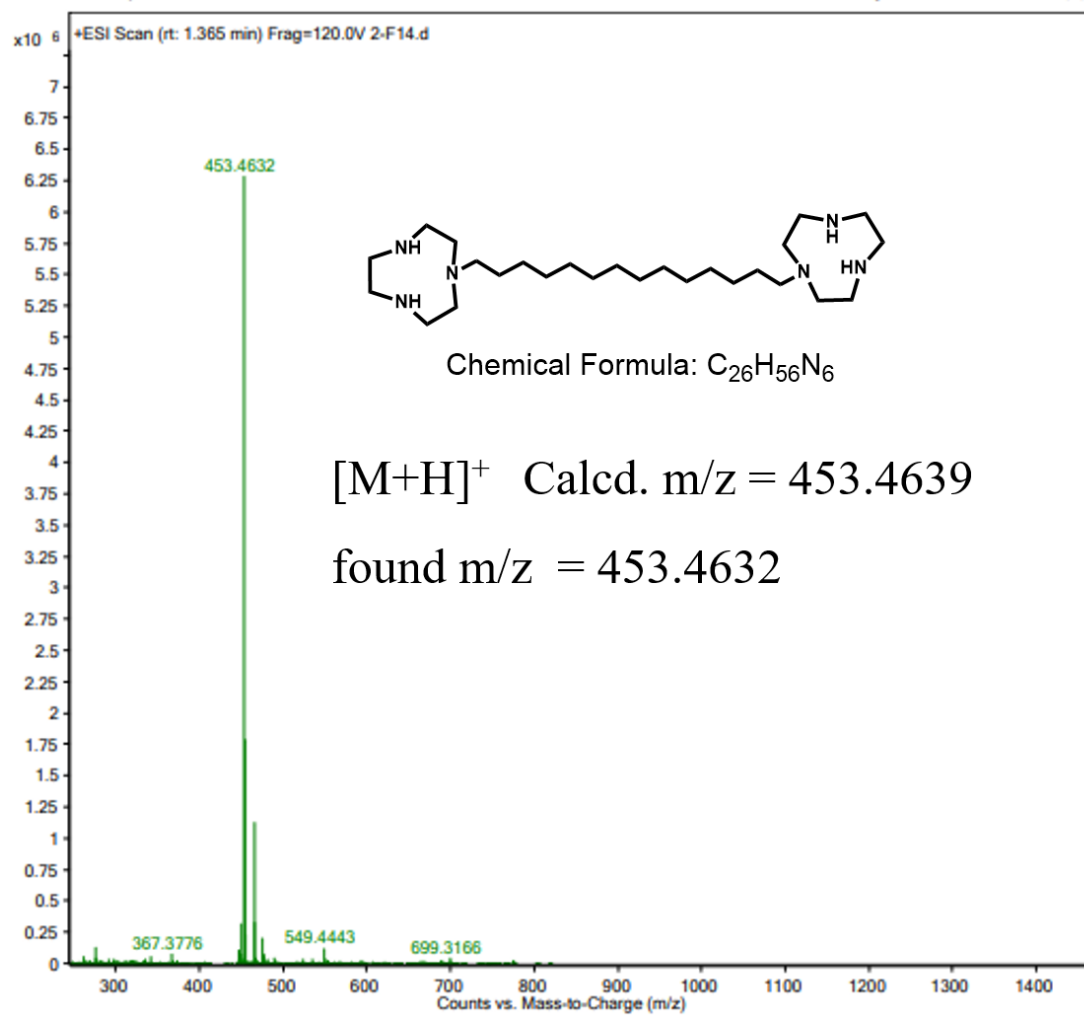


Figure S50. ESI-MS of TACN-C₁₄-TACN

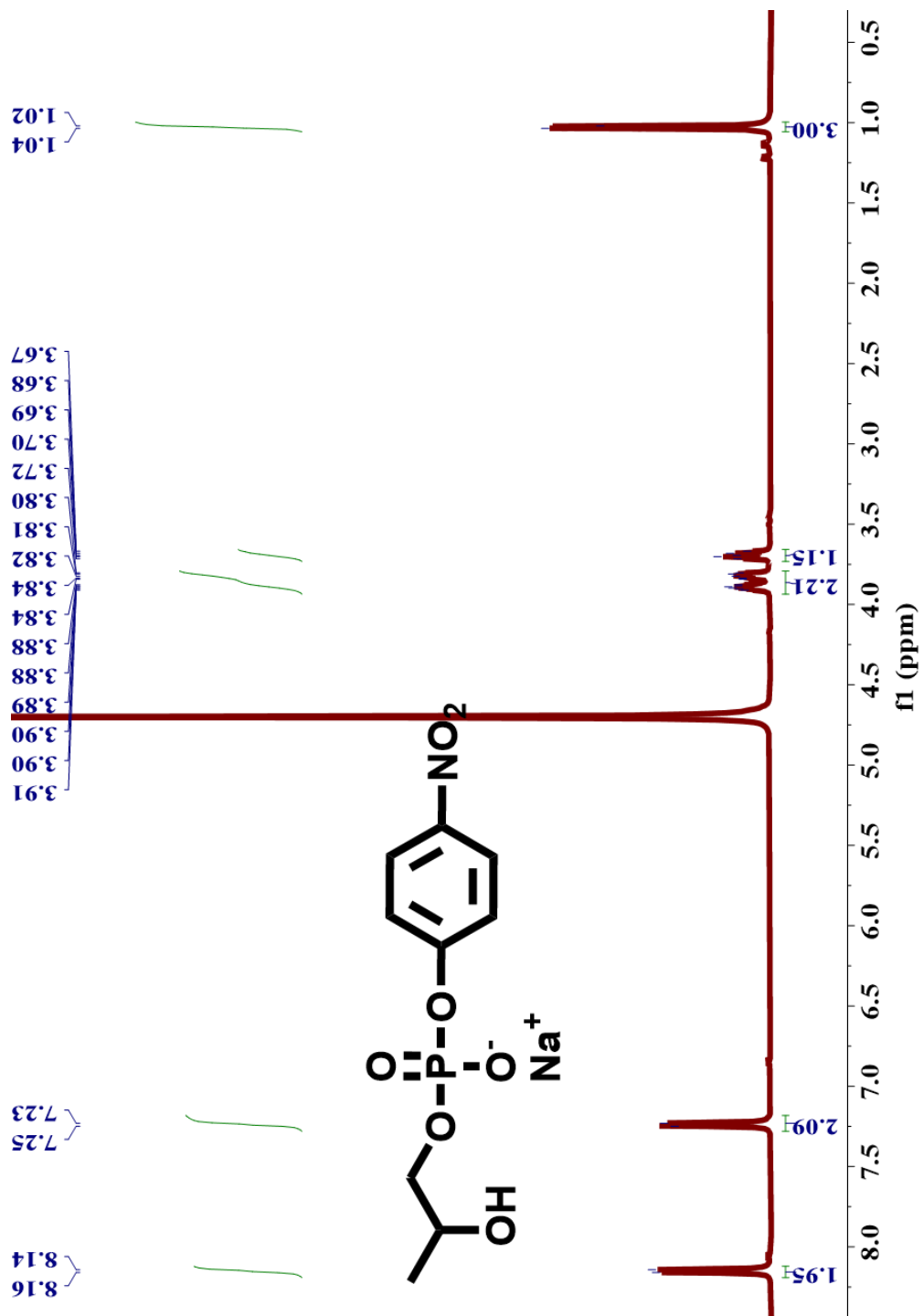


Figure S51. ¹H NMR of HPNP

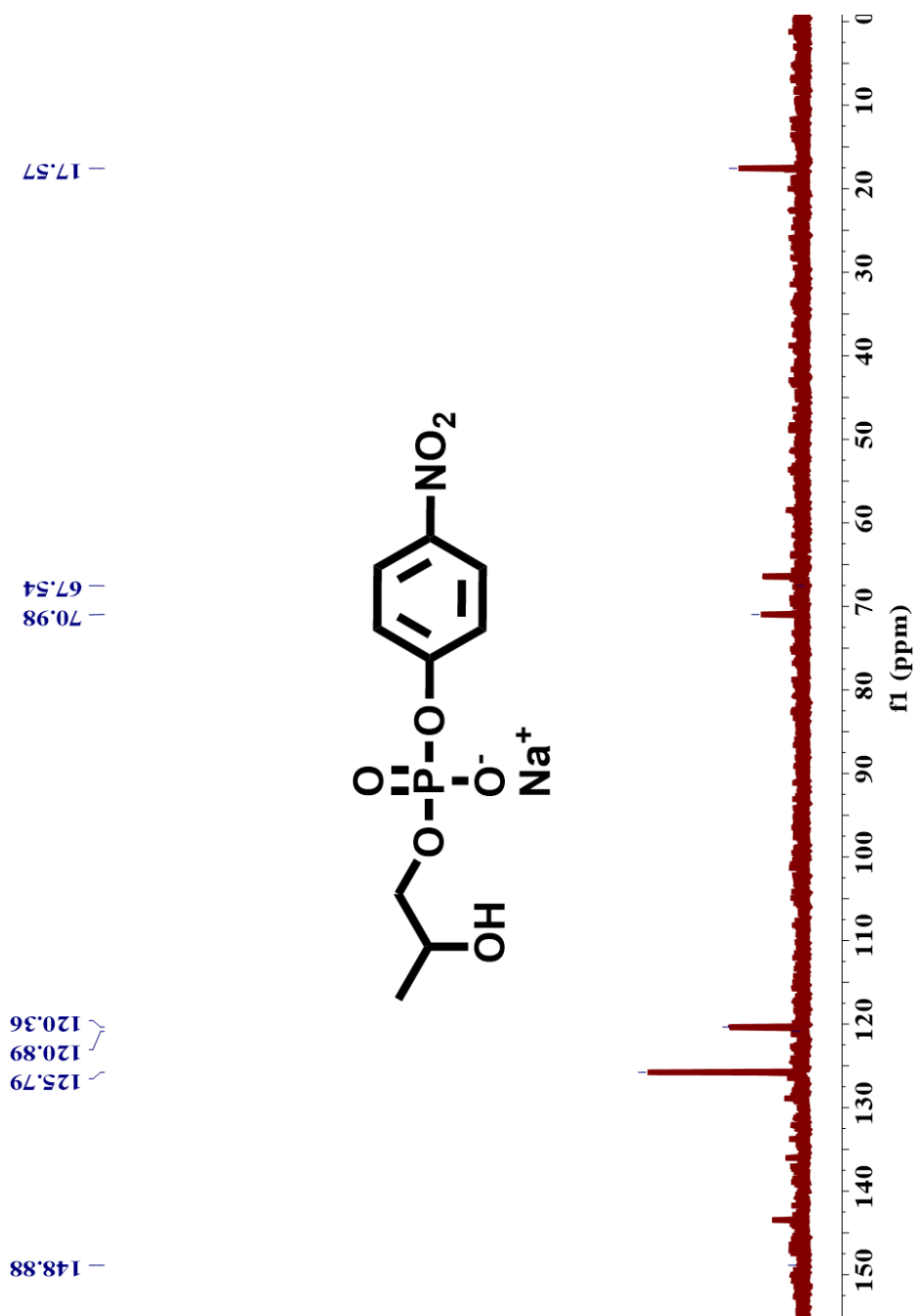


Figure S52. ¹³C NMR of HPNP

-4.89

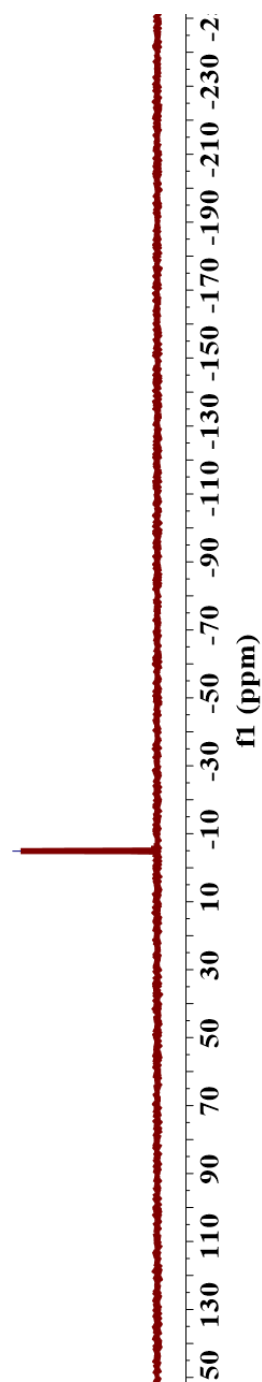
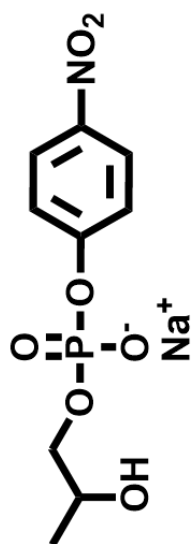


Figure S53. ^{31}P NMR of HPNP

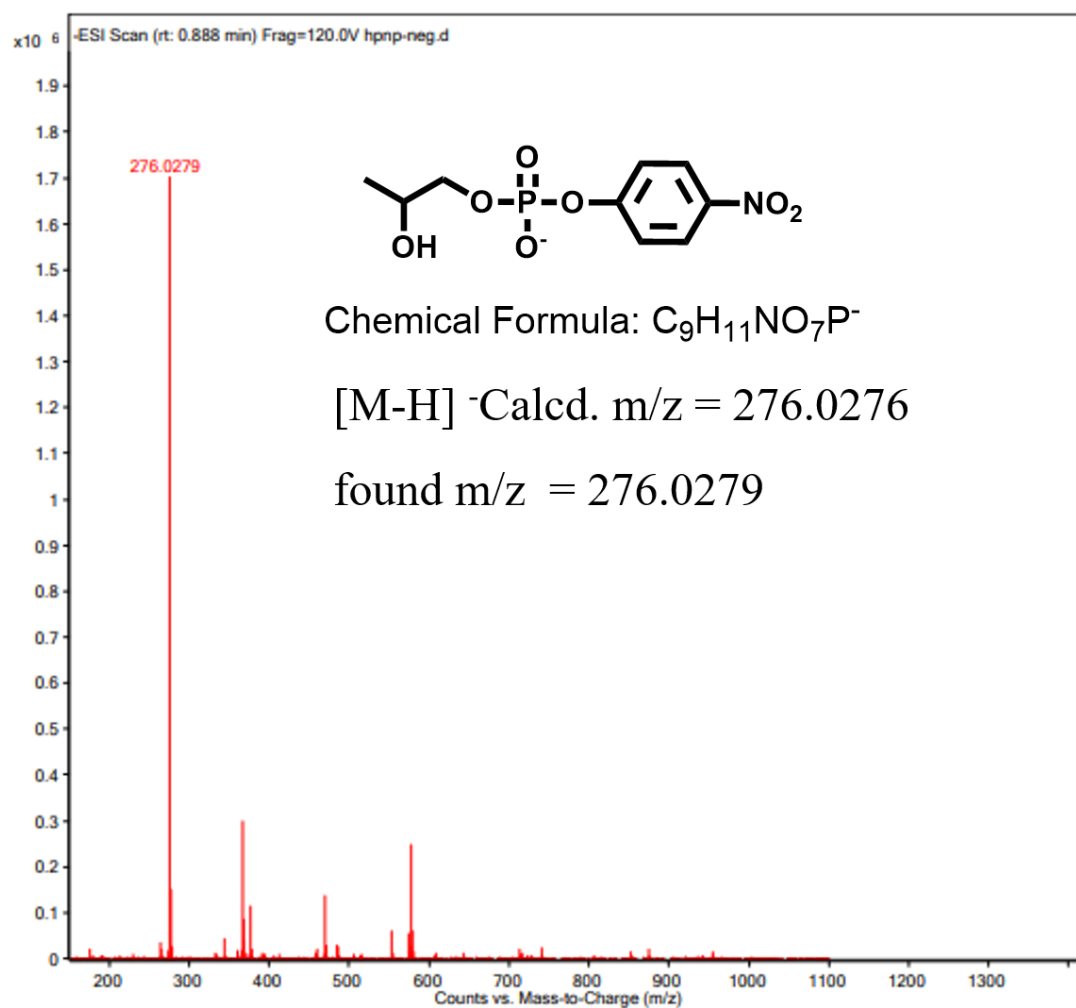


Figure S54. ESI-MS of HPNP